

848, 518 cm^{-1} ; HRMS (FAB) $[M + H]^+$ calcd for $\text{C}_{10}\text{H}_{12}\text{O}_4$ 322.9780, found 322.9791; $[\alpha]^{25}_{\text{D}} + 206$ (c 1.35, MeOH).

(4R,6R,7S)-9,9-Dimethyl-2-(E)-propenyl-5,8,10-trioxatricyclo[5.4.0.0^{4,6}]undec-1-en-3-one ((+)-20). To a solution of iodoenone (+)-8 (8.0 mg, 0.025 mmol), (E)-propenyl borate (6.6 mg, 0.077 mmol), Ag_2O (18.4 mg, 0.079 mmol) and Ph_3As (1.5 mg, 0.0050 mmol) in $\text{THF-H}_2\text{O}$ (10:1, 0.5 mL) was added $\text{Pd}(\text{PhCN})_2\text{Cl}_2$ (1.0 mg, 0.0025 mmol) and stirred at room temperature for 11 h in the dark. To the reaction mixture was added saturated NH_4Cl (aq) (2 mL) and stirred for 1 h at that temperature. The reaction mixture was filtered through a pad of Celite and organic materials were extracted with AcOEt (3 \times 10 mL). The combined organic phases were washed with brine and dried over Na_2SO_4 . The organic phase was concentrated in vacuo and the residue was purified by preparative thin-layer chromatography ($\text{Et}_2\text{O}/\text{benzene} = 1/6$) to afford dienone (+)-20 (4.5 mg, 77%) as a colorless oil. ^1H NMR (400 MHz, CDCl_3) δ 1.34 (3H, s), 1.51 (3H, s), 1.82 (3H, dd, $J = 6.5, 1.1$ Hz), 3.48 (1H, d, $J = 3.5$ Hz), 3.69 (1H, d, $J = 3.5$ Hz), 4.59 (1H, d, $J = 16.8$ Hz), 4.64 (1H, d, $J = 16.8$ Hz), 4.88 (1H, s), 5.89 (1H, qd, $J = 16.0, 6.5$ Hz), 6.06 (1H, d, $J = 16.0$ Hz); ^{13}C NMR (100 MHz, CDCl_3) δ 19.2, 24.8, 25.5, 53.1, 57.1, 63.0, 63.8, 101.5, 121.0, 127.9, 134.8, 148.7, 190.9; FT-IR (neat) ν 2989, 2931, 2854, 1682, 1385, 1373, 1238, 1082, 1038, 858 cm^{-1} ; HRMS (FAB) $[M + H]^+$ calcd for $\text{C}_{13}\text{H}_{17}\text{O}_4$ 236.1049, found 236.1053; $[\alpha]^{25}_{\text{D}} + 231$ (c 0.73, MeOH).

(1R,5S,6R)-5-Hydroxy-4-hydroxymethyl-3-(E)-propenyl-7-oxabicyclo[4.1.0]hept-3-en-2-one ((+)-7). To a solution of acetone (+)-20 (9.0 mg, 0.038 mmol) in MeOH (0.8 mL) was added Amberlyst 15 (9 mg), and the mixture was stirred at room temperature for 40 min. The reaction mixture was filtered, and the filtrate was concentrated in vacuo. The residue was purified by preparative thin-layer chromatography (AcOEt) to afford epoxycyclohexenol ((+)-7) (6.2 mg, 84%) as a colorless oil: ^1H NMR (400 MHz, CDCl_3) δ 1.84 (3H, dd, $J = 6.2, 1.0$ Hz), 2.10 (1H, bs), 3.13 (1H, bd, $J = 3.9$ Hz), 3.56 (1H, dd, $J = 3.9, 0.7$ Hz), 3.82 (1H, dd, $J = 3.9, 1.5$ Hz), 4.49 (1H, d, $J = 14.2$ Hz), 4.77 (1H, d, $J = 14.2$ Hz), 5.00 (1H, bs), 5.96 (1H, qd, $J = 16.0, 6.2$ Hz), 6.06 (1H, d, $J = 16.0$ Hz); ^{13}C NMR (100 MHz, CDCl_3) δ 19.2, 53.4, 55.6, 63.0, 65.2, 121.6, 131.0, 135.3, 146.3, 194.3; FT-IR (neat) ν 3371, 2916, 1676, 1444, 1373, 1051, 968, 868 cm^{-1} ; HRMS (FAB) $[M + H]^+$ calcd for $\text{C}_{10}\text{H}_{12}\text{O}_4$ 196.0736, found 196.0732; $[\alpha]^{25}_{\text{D}} + 285$ (c 0.41, MeOH).

Epoxyquinols A (1), B (2), and C (3) and Epoxytwinol A (4). To a solution of (+)-7 (78.9 mg, 0.402 mmol) in dry CH_2Cl_2 (8 mL) was added MnO_2 (700 mg, 75%, 6.03 mmol) at 0 $^\circ\text{C}$ under an argon atmosphere, and the mixture was stirred for 1 h at that temperature. The reaction mixture was filtered through a pad of Celite, washed with AcOEt , and then concentrated in vacuo. The residue was diluted with toluene (8 mL) and allowed to stand at room temperature for 10 h and purified by silica gel column and preparative thin-layer chromatography ($\text{MeOH}/\text{CHCl}_3 = 1/10$) to afford epoxyquinol A (1) (18.9 mg, 24%, colorless solid), epoxyquinol B (2) (25.0 mg, 33%, colorless oil), epoxyquinol C (3) (0.8 mg, 1%, colorless oil), and epoxytwinol A (4) (6.0 mg, 8%, colorless oil). **(1S,2R,4R,6R,7S,11S,12R,13S,16R,18R,19S,22R)-7,19-Dihydroxy-11,22-dimethyl-5,10,17,21-tetraoxaheptacyclo[11.7.2.0^{2,8}.0^{2,12}.0^{4,6}.0^{14,20}.0^{16,18}]docosa-8,14(20)-diene-3,15-dione (Epoxyquinol A (1)):** ^1H NMR (400 MHz, acetone- d_6) δ 0.71 (3H, d, $J = 6.2$ Hz), 1.00 (3H, d, $J = 6.7$ Hz), 2.44 (1H, bd, $J = 1.3$ Hz), 3.10 (1H, bd, $J = 1.4$ Hz), 3.38 (1H, d, $J = 3.6$ Hz), 3.43 (1H, bd, $J = 4.5$ Hz), 3.70–3.76 (2H, m), 4.30 (1H, qd, $J = 6.2, 1.2$ Hz), 4.42 (1H, qd, $J = 6.7, 1.0$ Hz), 4.63 (1H, bd, $J = 8.8$ Hz), 4.69 (1H, bd, $J = 8.8$ Hz), 4.89–4.97 (2H, m), 5.23 (1H, s), 6.73 (1H, d, $J = 1.7$ Hz); ^{13}C NMR (100 MHz, acetone- d_6) δ 20.3, 20.9, 38.1, 39.3, 50.7, 53.6, 56.3, 58.8, 63.9, 64.2, 66.7, 67.0, 72.4, 74.8, 115.1, 134.4, 142.5, 153.5, 190.2, 200.7; $[\alpha]^{25}_{\text{D}} + 63.1$ (c 0.945, MeOH), lit.²⁾ $[\alpha]^{25}_{\text{D}} + 61.0$ (c 0.146, MeOH).

(1S,2S,4R,6R,7S,11R,12S,13S,16R,18R,19S,22R)-7,19-Dihydroxy-11,22-dimethyl-5,10,17,21-tetraoxaheptacyclo[11.7.2.0^{2,8}.0^{2,12}.0^{4,6}.0^{14,20}.0^{16,18}]docosa-8,14(20)-diene-3,15-dione (Epoxyquinol B (2)): ^1H NMR (400 MHz, acetone- d_6) δ 0.73 (3H, d, $J = 6.4$ Hz), 1.27 (3H, d, $J = 6.4$ Hz), 2.79 (1H, dd, $J = 8.6, 3.0$ Hz), 3.12 (1H, dd, $J = 3.0, 1.0$ Hz), 3.31 (1H, dq, $J = 8.6, 6.4$ Hz), 3.48 (1H, dd, $J = 3.1, 0.7$ Hz), 3.50 (1H, dd, $J = 3.9, 0.8$ Hz), 3.66 (1H, dd, $J = 3.1, 1.8$ Hz), 3.85 (1H, dd, $J = 3.6, 1.6$ Hz), 4.04 (1H, qd, $J = 6.4, 1.0$ Hz), 4.60 (1H, bs), 4.81 (1H, bs), 5.18 (1H, s), 5.78 (1H, bs), 5.84 (1H, bs), 6.61 (1H, s); ^{13}C NMR (100 MHz, acetone- d_6) δ 19.6, 20.5, 36.9, 42.2, 53.0, 53.3, 53.3, 55.4, 57.0, 64.4, 68.6, 70.5, 73.7, 74.9, 107.0, 133.0, 150.9, 151.9, 191.9, 200.0; $[\alpha]^{25}_{\text{D}} + 151$ (c 0.710, MeOH); lit.³⁾ $[\alpha]^{25}_{\text{D}} + 153$ (c 0.315, MeOH).

(1R,2R,4R,6R,7S,11S,12R,13R,16R,18R,19S,22S)-7,19-Dihydroxy-11,22-dimethyl-5,10,17,21-tetraoxaheptacyclo[11.7.2.0^{2,8}.0^{2,12}.0^{4,6}.0^{14,20}.0^{16,18}]docosa-8,14(20)-diene-3,15-dione (Epoxyquinol C (3)): ^1H NMR (400 MHz, acetone- d_6) δ 0.72 (3H, d, $J = 6.4$ Hz), 1.14 (3H, d, $J = 6.4$ Hz), 3.06 (1H, dd, $J = 8.0, 3.0$ Hz), 3.12 (1H, dd, $J = 2.9, 1.2$ Hz), 3.31 (1H, dq, $J = 7.9, 6.4$ Hz), 3.47 (1H, dd, $J = 3.5, 1.0$ Hz), 3.49 (1H, bd, $J = 3.6$ Hz), 3.80 (1H, d, $J = 3.6$ Hz), 3.83 (1H, dd, $J = 3.5, 1.0$ Hz), 3.97 (1H, qd, $J = 6.4, 1.2$ Hz), 4.57 (1H, bs), 5.00 (2H, bs), 5.27 (1H, s), 5.59 (1H, s), 6.64 (1H, d, $J = 1.9$ Hz).

(1S,2S,4S,5R,7R,10S,11S,14R,16R,17S,20R,22R)-4,17-Dihydroxy-20,22-dimethyl-6,15,19,21-tetraoxaheptacyclo[9.7.2.2¹⁰.0^{3,9}.0^{5,7}.0^{12,16}.0^{14,16}]docosa-3(9),12(18)-diene-8,13-dione (Epoxytwinol A (4)): ^1H NMR (270 MHz, acetone- d_6) δ 0.77 (6H, d, $J = 6.2$ Hz), 3.21 (2H, bs), 3.53 (2H, dd, $J = 3.7, 1.0$ Hz), 3.85 (2H, dd, $J = 3.7, 1.0$ Hz), 4.20 (2H, q, $J = 6.4$ Hz), 4.38 (2H, d, $J = 9.7$ Hz), 4.60 (2H, bd, $J = 9.7$ Hz), 4.80 (2H, s).

(1S,2S,4R,6R,7S,11R,12S,13S,16R,18R,19S,22R)-7-Hydroxy-19-methoxy-11,22-dimethyl-5,10,17,21-tetraoxaheptacyclo[11.7.2.0^{2,8}.0^{2,12}.0^{4,6}.0^{14,20}.0^{16,18}]docosa-8,14(20)-diene-3,15-dione (21). To a solution of epoxyquinol B (3.0 mg, 0.0077 mmol) and iodomethane (48 μL , 0.77 mmol) in CH_3CN (0.5 mL) was added Ag_2O (90 mg, 0.39 mmol), and the mixture was stirred at room temperature for 5 h in the dark. The reaction mixture was filtered through a pad of Celite and washed with AcOEt . The filtrate was concentrated in vacuo, and the residue was purified by preparative thin-layer chromatography (AcOEt) to afford a 7:1 mixture of 3-methoxy epoxyquinol B (21) and 13-methoxy epoxyquinol B (22) (3.1 mg, 100%, colorless solid): ^1H NMR (400 MHz, CDCl_3) δ 0.78 (3H, d, $J = 6.4$ Hz), 1.27 (3H, d, $J = 6.4$ Hz), 2.76 (1H, dd, $J = 6.1, 2.7$ Hz), 3.12 (1H, br-d, $J = 2.5$ Hz), 3.46 (1H, d, $J = 3.2$ Hz), 3.54 (3H, s), 3.55–3.60 (2H, m), 3.66 (1H, br-t, $J = 2.6$ Hz), 3.88 (1H, d, $J = 3.5$ Hz), 4.18 (1H, br-q, $J = 6.4$ Hz), 4.25 (1H, s), 4.53 (1H, br-d, $J = 1.8$ Hz), 4.68 (1H, s), 5.13 (1H, s) 6.43 (1H, s); ^{13}C NMR (100 MHz, CDCl_3) δ 19.5, 19.9, 37.3, 42.0, 52.5, 52.7, 54.1, 54.7, 55.9, 67.6, 70.6, 72.4, 73.0, 74.2, 78.3, 107.1, 135.2, 146.3, 148.6, 189.9, 199.3; HRMS (FAB) $[M + H]^+$ calcd for $\text{C}_{21}\text{H}_{23}\text{O}_8$ 403.1393, found 403.1399.

(1S,2S,4R,6R,7S,11R,12S,13S,16R,18R,19S,22R)-19-Hydroxy-7-methoxy-11,22-dimethyl-5,10,17,21-tetraoxaheptacyclo[11.7.2.0^{2,8}.0^{2,12}.0^{4,6}.0^{14,20}.0^{16,18}]docosa-8,14(20)-diene-3,15-dione (22). A solution of 3-methoxy epoxyquinol B and 13-methoxy epoxyquinol B (7:1 mixture, 1.5 mg) in 2-propanol (0.5 mL) was refluxed for 36 h. The reaction mixture was concentrated in vacuo to afford 3.5:1 mixture of 22 and 21: ^1H NMR (400 MHz, CDCl_3) δ 0.79 (3H, d, $J = 6.4$ Hz), 1.33 (3H, d, $J = 6.3$ Hz), 2.86 (1H, dd, $J = 8.9, 3.1$ Hz), 3.11 (1H, br-d, $J = 3.0$ Hz), 3.29 (1H, dq, $J = 8.9, 6.3$ Hz), 3.48–3.53 (2H, m), 3.71 (3H, s), 3.73 (1H, dd, $J = 2.9, 1.3$ Hz), 3.82 (1H, dd, $J = 3.6, 1.3$ Hz), 4.10 (1H, br-q, $J = 6.4$ Hz), 4.11 (1H, s), 4.76 (1H, s), 4.88 (1H, s), 5.06 (1H, d, $J = 1.3$ Hz) 6.60 (1H, s); ^{13}C NMR (100 MHz, CDCl_3) δ 19.2, 20.2, 35.9, 41.0, 51.0, 52.4, 52.6, 56.1, 58.0, 63.4, 63.8, 69.7, 72.8, 74.6, 78.3, 103.5, 132.3, 150.6, 152.4, 190.9, 197.9.

General Procedure of Table 4. To a solution of alcohol **25** (5.0 mg, 0.030 mmol) in dry CH_2Cl_2 (0.3 mL) was added MnO_2 (209 mg, 75%, 1.80 mmol) at 0 °C under an argon atmosphere, and the mixture was stirred for 1 h at that temperature. The reaction mixture was filtered through a pad of Celite, washed with AcOEt, and then concentrated at 0 °C in vacuo. To the residue was added methyl vinyl ketone (0.25 mL, 3.0 mmol), and the mixture was allowed to stand at room temperature for 10 h. The mixture was concentrated in vacuo and purified by preparative thin-layer chromatography (AcOEt/hexane = 1/1) to afford **28a** (5.2 mg, 76%, colorless oil).

rel-(1S,8R,10R,12S)-12-Acetyl-10-methyl-9-oxatricyclo[6.2.2.0^{2,7}]dodec-2(7)-en-3-one (28a): ^1H NMR (400 MHz, CDCl_3) δ 0.84 (3H, d, $J = 6.1$ Hz), 1.26 (1H, ddd, $J = 12.3, 6.5, 2.6$ Hz), 1.97–2.20 (6H, m), 2.44 (2H, t, $J = 6.6$ Hz), 2.57 (2H, t, $J = 6.0$ Hz), 3.19 (1H, bs), 3.29–3.39 (1H, m), 3.95 (1H, q, $J = 6.1$ Hz), 4.46 (1H, d, $J = 3.0$ Hz); ^{13}C NMR (100 MHz, CDCl_3) δ 21.1, 23.1, 27.3, 28.4, 29.7, 31.4, 37.4, 51.7, 70.2, 72.1, 134.7, 161.2, 195.8, 207.7; FT-IR (neat) ν 2966, 2925, 2864, 1712, 1664, 1456, 1194, 1173, 1014, 876 cm^{-1} ; HRMS (FAB) $[\text{M} + \text{H}]^+$ calcd for $\text{C}_{14}\text{H}_{19}\text{O}_3$ 235.1334, found 235.1327.

rel-(1S,2S,10R,11S,12S,20R)-10,20-Dimethyl-9,19-diphenyl-9,19-diazapentacyclo[10.6.2.0^{2,7}.0^{2,11}.0^{13,18}]icosa-7,13-(18)-diene-3,14-dione (32). To a solution of alcohol **25** (42.0 mg, 0.253 mmol) in dry CH_2Cl_2 (1.0 mL) was added MnO_2 (1.17 g, 75%, 10.1 mmol) at 0 °C under an argon atmosphere, and the mixture was stirred for 1 h at that temperature. The reaction mixture was filtered through a pad of Celite, washed with AcOEt, and then concentrated at 0 °C in vacuo. To the residue was added aniline (0.47 mL, 5.1 mmol), and the mixture was allowed to stand at room temperature for 12 h. The mixture was concentrated in vacuo and purified by alumina column chromatography (AcOEt/hexane = 1/10) and further recrystallization from AcOEt to afford azapentacycle **32** (18.1 mg, 30%, yellow prisms): mp 197.0–198.0 °C (dec);

^1H NMR (400 MHz, CDCl_3) δ 0.79 (3H, d, $J = 6.0$ Hz), 1.00 (3H, d, $J = 6.7$ Hz), 1.68 (1H, qt, $J = 13.6, 4.0$ Hz), 1.93–2.27 (5H, m), 2.33–2.42 (2H, m), 2.56 (1H, ddd, $J = 18.0, 7.9, 5.0$ Hz), 2.63–2.80 (3H, m), 3.27 (1H, s), 3.40 (1H, s), 3.94 (1H, qd, $J = 6.0, 2.1$ Hz), 3.99 (1H, q, $J = 6.7$ Hz), 5.20 (1H, s), 6.18 (1H, s), 6.64 (1H, t, $J = 7.2$ Hz), 6.72 (4H, d, $J = 7.2$ Hz), 6.82 (1H, t, $J = 7.2$ Hz), 7.15 (2H, t, $J = 7.5$ Hz), 7.21 (2H, t, $J = 7.5$ Hz); ^{13}C NMR (100 MHz, CDCl_3) δ 16.6, 16.8, 22.9, 27.6, 29.2, 29.4, 37.0, 39.4, 40.5, 43.9, 52.7, 53.8, 58.9, 59.2, 113.8, 113.8, 114.1, 117.1, 119.7, 125.1, 129.3, 129.3, 133.6, 144.7, 145.4, 156.5, 195.2, 206.0; FT-IR (film) ν 3058, 2968, 2929, 2864, 1705, 1668, 1595, 1504, 1404, 1246, 1030, 748, 694 cm^{-1} ; HRMS (FAB) $[\text{M} + \text{H}]^+$ calcd for $\text{C}_{32}\text{H}_{35}\text{N}_2\text{O}_2$ 479.2699, found 479.2693.

Acknowledgment. The authors thank Meito Sangyo Co. for the generous gift of several lipases. The authors are indebted to Professor Takeshi Sugai of Keio University for his invaluable suggestions concerning the kinetic resolution by lipase. The authors are grateful to Shinetsu-Kagaku Corporation for the gift of TBSCl. This work was supported by a Grand-in-Aid for Scientific Research on Priority Areas (A) "Creation of Biologically Functional Molecules" from the Ministry of Education, Culture, Sports, Science and Technology, Japan.

Supporting Information Available: Full characterization of compound **24** and **28**, ORTEP drawing of compound **32**, and copies of ^1H and ^{13}C NMR and IR of all new compounds. This material is available free of charge via the Internet at <http://pubs.acs.org>.

JO048425H

新しい血管新生阻害剤におけるケミカルゲノミクス

Ho Jeong Kwon / 訳：掛谷秀昭

さまざまな遺伝子の機能探索や医薬品の開発を促進するため低分子化合物を利用する“ケミカルゲノミクス”は、化学と生物学の学際的な研究を推進するのに強力な手段となる。細胞膜透過性をもち標的蛋白質に結合するような生理活性低分子化合物(生理活性をもつ低分子有機化合物)は、細胞や微生物の表現型に変化を誘導することができる。これらの標的蛋白質は、アフィニティー法や遺伝学的手法、あるいはプロテオミクス的手法を駆使して同定することが可能である。さらに、低分子化合物による標的蛋白質の特異的な分子認識機構を解明することは、その作用機構を理解し、構造活性相関に基づきすぐれた医薬品を開発するための近道ともなりうる。このような考えのもと、筆者らは、ケミカルゲノミクスを血管新生に応用し、新しい血管新生阻害剤の開発とそれらの標的蛋白質の同定を行なっている。

Key words ケミカルゲノミクス 血管新生阻害剤 化合物ライブラリー スクリーニング ファージディスプレイ

はじめに

ケミカルゲノミクス (chemical genomics/genetics, 化学遺伝学) は、化学と生物学におけるツールと技術の融合により、遺伝子の機能探索や医薬品の開発を促進する新しい研究パラダイムであり¹⁻⁵⁾、フォワードケミカルゲノミクスとリバースケミカルゲノミクスに分類される(図1)。表1に、生理活性低分子化合物と、ケミカルゲノミクスのアプローチによって同定されたその標的分子の一例を示す⁶⁻¹¹⁾。ある低分子化合物の標的蛋白質が同定されれば、その低分子化合物は標的蛋白質の機能を研究するためのユニークなツールとなるのみならず、新しい医薬品開発のためのリード化合物となる可能性をも秘めている。さらに、この標的蛋白質は特定の疾病の治療標的ともなりうるため、ケミカルゲノミクスは製薬企業において医薬品開発のための有用な方法論として利用されている¹²⁻¹⁴⁾。

本稿では、筆者らが進めている、新しい血管新生阻害剤の開発にむけてのケミカルゲノミクス研究を紹介する。

表1 生理活性低分子化合物と、ケミカルゲノミクスのアプローチによって同定されたその標的蛋白質

生理活性低分子化合物	生理活性	標的蛋白質
FK506	免疫抑制剤	FKBP
ラバマイシン	免疫抑制剤	mTOR
レプトマイシン	細胞周期阻害剤	Crm1
ラクタシスチン	細胞周期阻害剤	20S プロテアソーム
トラボキシン	抗癌剤	ヒストンデアセチラーゼ
フマギリン	血管新生阻害剤	MetAP-2
ラディシコール	抗癌剤	HSP90
エポネマイシン	抗癌剤	20S プロテアソーム
ミリオシン	免疫抑制剤	LCB1, LCB2
パルセノライド	抗炎症剤	IκB キナーゼ
ドキシソルピジン	抗癌剤	hNopp140

Ho Jeong Kwon, Chemical Genomics National Research Laboratory, Department of Bioscience and Biotechnology, Sejong University E-mail: kwonhj@sejong.ac.kr http://dasan.sejong.ac.kr/~cgml/

Hideaki Kakeya, 理化学研究所中央研究所 長田抗生物質研究室 E-mail: hkakeya@riken.jp http://www.antibiotics.riken.go.jp/japanese/staff/kakeya/kakeya.html

Chemical genomics on new angiogenesis inhibitors

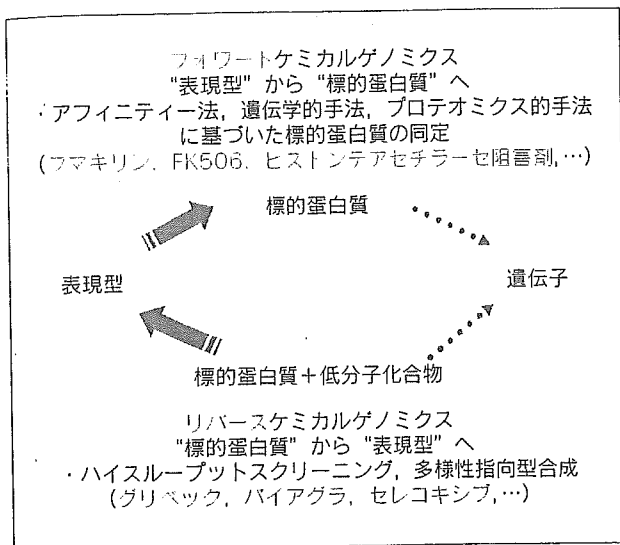


図1 ケミカルゲノミクスの概略

フォワードケミカルゲノミクスは、細胞や微生物において特異的な表現型を示す活性をもつ低分子化合物を出発点とし、そのうち、アフィニティー法、遺伝学的手法、あるいはプロテオミクス的手法により、その低分子化合物の標的蛋白質を同定する方法論である。一方、リバースケミカルゲノミクスは、フォワードケミカルゲノミクスやほかのオミクス(-omics, 網羅的解析を意味する)を基盤とした研究により得られた標的蛋白質を出発点とし、ハイスループットスクリーニング、あるいは構造に基づいたドラッグデザインにより、新しい医薬品候補となるような低分子化合物を見いだす方法論である。

I. 血管新生におけるケミカルゲノミクスの応用

血管新生は内皮細胞によって新しい血管が形成される過程である¹⁵⁾。この過程は非常に複雑で、内皮細胞によって分泌される蛋白質分解酵素による細胞膜の分解、刺激による化学遊走、内皮細胞の増殖、管腔形成など、多岐にわたるステップを含んでいる^{16,17)}。これらおのおの過程は、血管新生の促進因子および阻害因子によって厳密に制御されている。しかし、癌をはじめとした多くの疾病において、これら精巧な制御機構はしばしば破綻している。最近の多くの研究結果から、この血管新生が癌細胞の異常増殖やほかの組織への転移のための重要なステップであることが示されている¹⁸⁾。したがって、血管新生を特異的に阻害することは、癌の増殖や転移を抑制する強力な手法として期待されている(図2)。

血管新生に重要な蛋白質の同定にむけて多くの研究がなされており、マトリックスメタロプロテアーゼ¹⁹⁾、血管内皮増殖因子受容体²⁰⁾、などがその例である。しかし

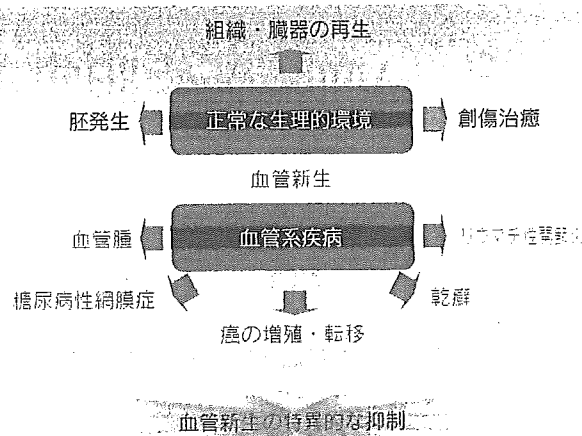


図2 医薬品開発における血管新生の重要性

血管新生は、内皮細胞によって新しい血管が形成される複数の過程からなり、胚発生や創傷治癒などのような正常な生理条件下において重要である。病的条件下においては、その制御機構が破綻し、多くの血管新生促進因子によって血管新生が促進されて、糖尿病性網膜症、リウマチ性関節炎、乾癬、癌の増殖・転移など、さまざまな疾病が誘導される。その厳密な制御機構の破綻は、癌を含む多くの疾病の進展過程において、管腔のネットワーク形成も病的な状態とする。したがって、病的な血管新生を特異的に抑制することは、癌の増殖や転移を抑制するための強力な方法と考えられる。

残念なことに、これらの蛋白質を阻害する薬剤は、*in vivo*における複雑な血管新生を阻害するのに十分な活性をもっていない、あるいは、血管新生に関連した標的蛋白質に特異的でないなど、さまざまな理由により臨床薬までには至っていない²¹⁾。したがって、細胞レベルで血管新生過程を阻害可能な新薬の開発の必要性和、後期臨床試験におけるリスク減少の必要性はますます増大しており、そのためケミカルゲノミクスを基盤とした血管新生に関する研究の重要性が高まっている。これまで、いくつかの化学構造的には関連性のない低分子化合物が、内皮細胞に対し表現型の変化を誘導する血管新生阻害剤として単離されている²²⁻²⁵⁾。血管新生阻害剤の標的蛋白質の同定と評価のためのケミカルゲノミクスの応用は、血管新生の基盤となる複雑な分子機構の解明にも新しい知見を与えつつある。さらに、血管新生抑制療法のための新しい標的蛋白質とリード化合物もまた生み出されつつある。

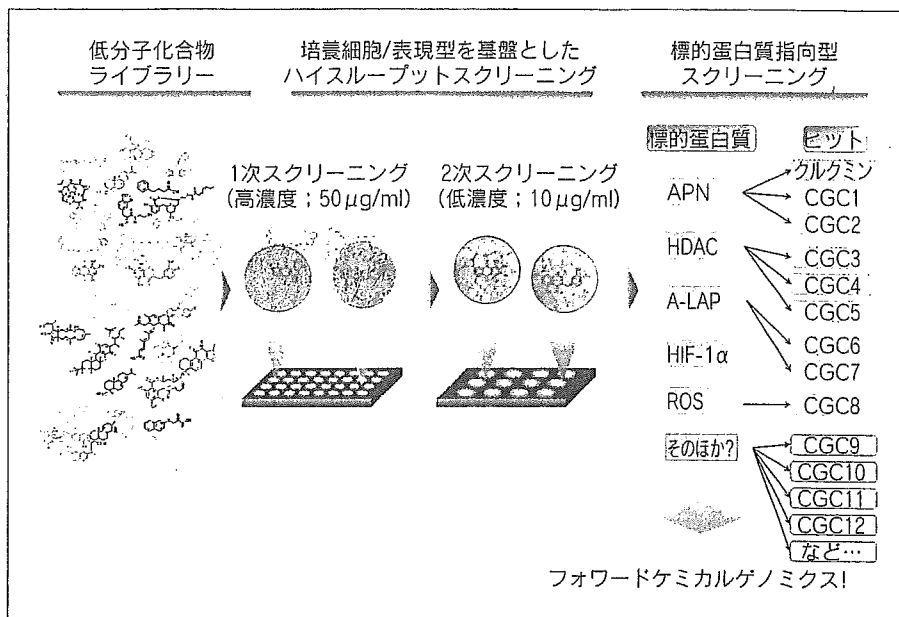


図3 血管新生に対するケミカルゲノミクスの概略

天然有機化合物および合成化合物からなる低分子化合物ライブラリーを、内皮細胞を用いたスクリーニング系に適用した。1次スクリーニングとして増殖阻害活性を検討し、2次スクリーニングとして内皮細胞による管腔形成に与える影響を検討して、活性化合物を評価した。そして、既存の血管新生関連蛋白質に与える影響を検討するとともに、フォワードケミカルゲノミクスの手法により標的蛋白質の同定を行なった。

II. クルクミンはアミノペプチダーゼNを阻害し血管新生を抑制する

筆者らは、血管新生におけるケミカルゲノミクスを基盤とした研究を行なうため、独自の化合物ライブラリーを作成し、また、内皮細胞を利用する評価系を確立した(図3)。これにより新規血管新生阻害剤をスクリーニングした結果、ウコン *Curcuma longa* のメタノール抽出液に、内皮細胞の増殖と内皮細胞の示す明確な表現型である管腔形成を阻害する活性を見いだした。そして、その粗抽出液より活性物質を精製し、活性本体としてクルクミンを再発見した。クルクミンは、ウコンの根茎から単離・精製された芳香環をもつ天然有機化合物であり、その構造には2組みの α 、 β -不飽和カルボニル基が含まれている。現在、クルクミンは、米国立癌研究所(NCI)において癌の強力な化学予防薬として第1相臨床試験が行なわれている²⁶⁾。ほかの多くの研究機関もクルクミンの第1相臨床試験の結果を報告しており、薬理学的に安全で癌の予防と治療に非常に効果的であるという有望な結果が示されている²⁷⁾。クルクミンのもつ化学予防活性はさまざまなタイプの癌種に及び²⁸⁾、その顕著な活性は血管新生の直接的な抑制に起因している可能性が示唆されて²⁹⁾、この効果が *in vivo* においても腫瘍の増大を効果的に抑制する要因であることが考えられる³⁰⁾。しかし、これまでにクルクミンによる血管新生阻害機構の詳

細は明らかにされていなかった。

クルクミンの血管新生阻害活性の標的蛋白質を同定するため、アミノペプチダーゼN、脂肪細胞由来ロイシンアミノペプチダーゼ、ヒストンデアセチラーゼ、低酸素誘導因子(HIF)など、血管新生に重要な複数の既知蛋白質に対するクルクミンの効果を検討した。その結果、興味深いことに、クルクミンはアミノペプチダーゼNに結合し不可逆的にその活性を阻害することを見いだした。クルクミンとアミノペプチダーゼNとの直接的な相互作用は、表面プラズモン共鳴解析(図4a)と抗体による拮抗阻害実験により、*in vitro* レベルおよび *in vivo* レベルで確定された。

クルクミンとその誘導体のアミノペプチダーゼNへの可能な結合様式を、ドッキングモデルにより検討した。ここでは、ウシレンズ由来ロイシンアミノペプチダーゼ(EC.3.4.11.1)の活性部位のX線結晶構造³¹⁾を利用した。クルクミンは、アミノペプチダーゼNを阻害する濃度域でロイシンアミノペプチダーゼの酵素活性を同様に阻害した。ドッキングモデルにおいては、クルクミンはロイシンアミノペプチダーゼの触媒部位にうまくフィットした(図4b)。ロイシンアミノペプチダーゼの活性部位は、クルクミンとMichael反応あるいはシッフ塩基を形成可能な2つのリジン残基(Lys250, Lys262)を含んでいる。一方、構造的に固定されたヒドラジノクルクミンはロイシンアミノペプチダーゼの触媒部位へフィットできず(図4c)、また、アミノペプチダーゼN活性を

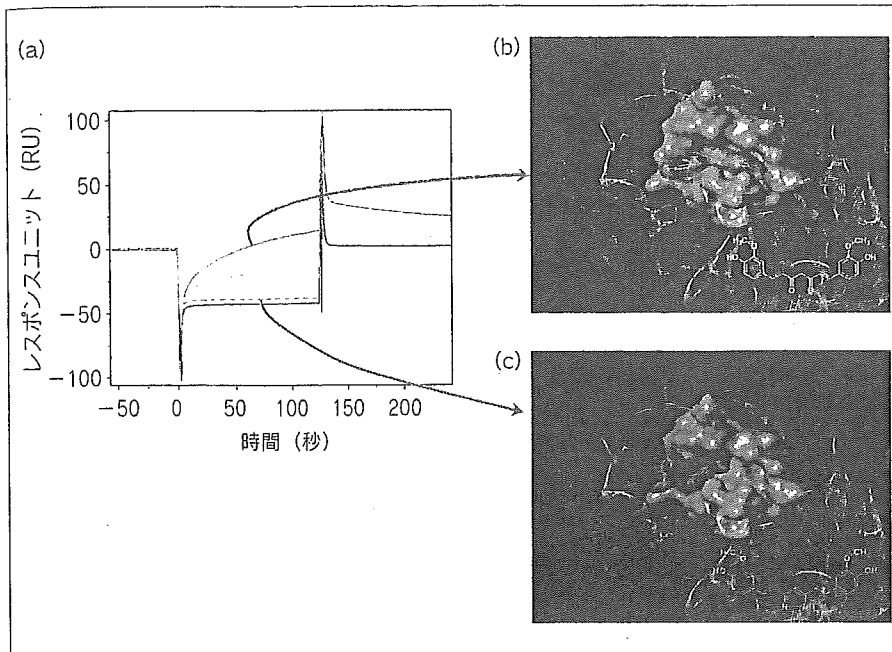


図4 アミノペプチダーゼNとクルクミンの相互作用と、ロイシニアミノペプチダーゼ活性部位におけるクルクミンのドッキングモデル

(a) 表面プラズモン共鳴解析の結果。4 μ Mクルクミン(緑色点線)、16 μ Mクルクミン(水色破線)、50 μ Mクルクミン(青色実線)、100 μ Mヒドロジノクルクミン(オレンジ色破線)、あるいは、5%ジメチルスルホキシド(黒色実線)をそれぞれ含む溶液を、アミノペプチダーゼNを固定化したセンサーチップ上に流すことで得たセンサーグラム。クルクミンだけにアミノペプチダーゼNとの相互作用がみられた。

(b) クルクミンとロイシニアミノペプチダーゼのドッキングモデル。FlexXプログラム(Sybyl 6.8.)を用いて作成した。クルクミン(緑色)は、ウシレンズ由来ロイシニアミノペプチダーゼの触媒部位にうまくフィットした。

(c) ヒドロジノクルクミンとロイシニアミノペプチダーゼのドッキングモデル。構造的に固定化された類縁化合物ヒドロジノクルクミン(紫色)は、ロイシニアミノペプチダーゼの触媒部位にフィットすることができない。

いて求核性のアミノ酸残基と共有結合しようと結論づけた。

プロテアーゼによる細胞基底膜の分解は、癌細胞の浸潤と転移に必須のステップである。アミノペプチダーゼNは亜鉛結合型マトリックスメタロプロテアーゼであり、癌細胞の浸潤と転移に深く関与している³³⁾。したがって、クルクミンのアミノペプチダーゼN活性阻害は、クルクミンが血管新生を抑制するのに十分であると考えられた^{34, 35)}。さらに筆者らは、アミノペプチダーゼNを阻害するのに必要な濃度域と同じ濃度域で、クルクミンがアミノペプチダーゼN陽性癌細胞の浸潤、および増殖因子が誘導する内皮細胞の血管新生を抑制することを見いだした。一方、クルクミンは、アミノペプチダーゼN陰性の乳癌細胞の浸潤は抑制しなかった。これらのデータから、アミノペプチダーゼNはクルクミンの抗浸潤活性の直接的な標的であることが示唆され

阻害できない。

いくつかの実験から、クルクミンの α 、 β -不飽和ケトン基が標的蛋白質への結合に重要であることが示唆された。興味深いことに、亜鉛結合型メタロペプチダーゼM1ファミリー(ブタアミノペプチダーゼN、ヒトアミノペプチダーゼN、ヒトアミノペプチダーゼA、ラットアミノペプチダーゼB、マウスピューロマイシン感受性アミノペプチダーゼなど)は、それらの活性部位内に非常によく保存された4つのドメインをもっている³²⁾。これら保存されたドメインには、2つの求核性のアミノ酸残基(Cys218, Lys225)がある。さらに筆者らは、チオール化合物でクルクミンを還元することでアミノペプチダーゼN阻害活性が完全に消失することを確認した。したがって筆者らは、クルクミンの α 、 β -不飽和カルボニル基が、アミノペプチダーゼNの活性部位にお

た。内皮細胞の浸潤は血管新生に必須であることを考慮すると、クルクミンの血管新生抑制活性もまた、部分的にはアミノペプチダーゼN活性の阻害に起因しているだろう。したがって筆者らは、血管新生に対するケミカルゲノミクス的手法により臨床的に有望な薬剤を見だし、また、アミノペプチダーゼNは血管新生において重要な蛋白質であることを見いだしたのである。

III. フォワードケミカルゲノミクスによるクルクミン類縁化合物HBCの標的蛋白質の同定

クルクミンおよびその複数の類縁化合物は、*in vivo*における血管新生阻害剤であることが知られている。クルクミンは薬理学的に安全な天然有機化合物であるので、クルクミンの化学構造は、フォーカストラライブラリー

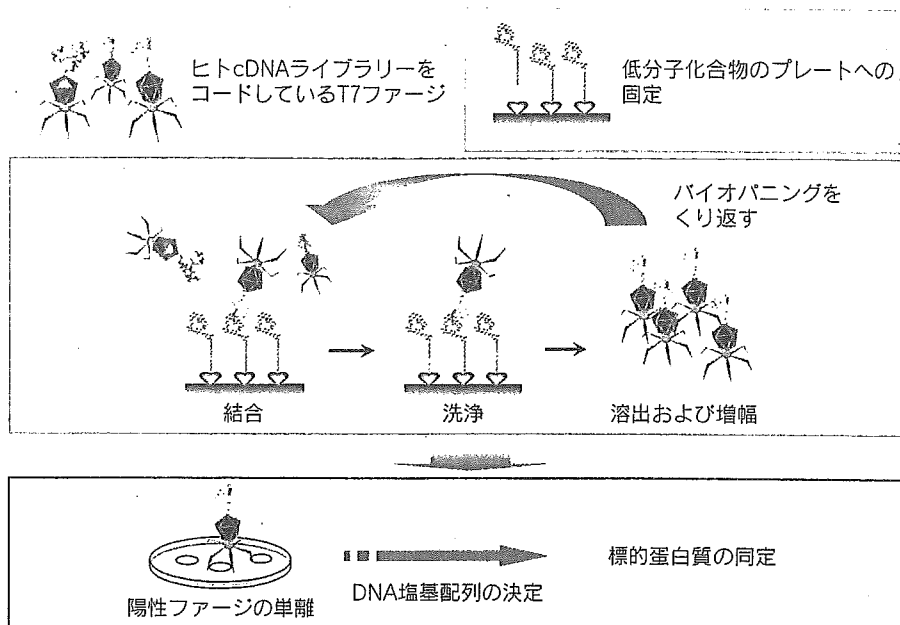


図5 ファージディスプレイ法の概略
ファージディスプレイ・バイオバニング法による低分子化合物の標的蛋白質の同定。

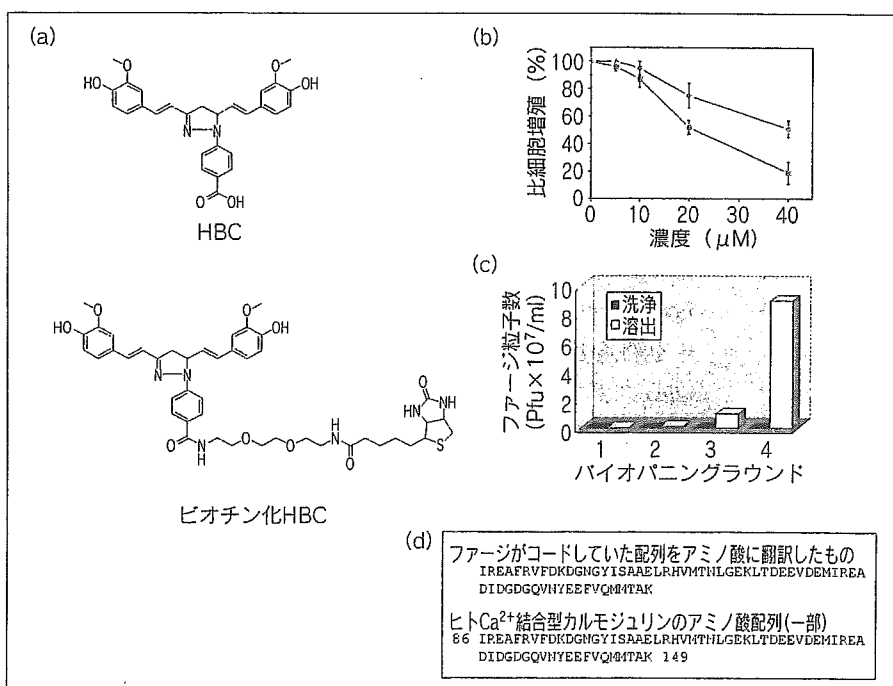


図6 ファージディスプレイ法によるHBCの標的蛋白質の同定

(a) HBCおよびビオチン化HBCの化学構造。

(b) HBC(■)およびビオチン化HBC(●)の、HCT15細胞における増殖抑制効果。細胞を各薬剤で72時間処理し、MTT法により生存数を評価した。

(c) 各バイオバニングラウンドの溶出されたHBCに結合したファージ粒子数。洗浄のところは、ストレプトアビジンでコートしたウェル上のビオチン化HBCに結合した、非特異的なファージ粒子の数を表す。

(d) HBCに結合したファージがコードする蛋白質と、ヒトCa²⁺結合型カルモジュリンとのあいだのアミノ酸配列同一性。このファージがコードする蛋白質は、ヒトCa²⁺結合型カルモジュリンのC末端(86~149)と完全に一致した。

[→今月のKey Words (p.1036)] を創製するための有益なファーマコアになりうる。この考えに基づき、筆者らはいくつかの新しいクルクミン類縁化合物を開発し、それらの生理活性を評価した²⁴⁾。それらの類縁化合物のなかで、4-{3,5-bis-[2-(4-hydroxy-3-methoxy-phenyl)-ethyl]-4,5-dihydro-pyrazol-1-yl}-benzoic acid (以下、

HBC) が複数のヒト癌細胞の増殖を強力に抑制することを見いだしたが、このHBCがどのように癌細胞の増殖を抑制するかについてはまったく不明であった。興味深いことに、HBCはクルクミンの結合蛋白質であるアミノペプチダーゼNの活性を阻害せず、HBCは細胞増殖に重要なほかの蛋白質を標的にしていることが示唆さ

れた。そこで筆者らは、フォワードケミカルゲノミクスによりHBCの標的蛋白質を同定することを試みた。

アフィニティマトリックスを利用する標的蛋白質の同定には、低分子化合物が標的蛋白質と高い親和性をもつことが要求される。HBCが生理活性をもつ濃度は約 $10\mu\text{M}$ であるので、アフィニティ法により標的蛋白質を同定するにはやや親和性が低いと思われた。それゆえ筆者らは、低親和性リガンドの標的蛋白質の同定が可能なファージディスプレイ法を利用した(図5)。ファージディスプレイ法では、細胞においてきわめて少ない内在性蛋白質を単離することが可能である³⁶⁾。

筆者らは、ビオチン化HBCを用いたファージディスプレイ法により、 Ca^{2+} 結合型カルモジュリンをHBCの直接的な標的蛋白質として単離した³⁷⁾(図6)。 Ca^{2+} 結合型カルモジュリンは、細胞増殖などさまざまな細胞機能に関与している Ca^{2+} 結合蛋白質である³⁸⁾。それ自身は触媒活性を示さないが、ミオシン軽鎖キナーゼ³⁹⁾、カルモジュリンキナーゼ⁴⁰⁾、ホスホジエステラーゼ⁴¹⁾、プロテインホスファターゼ⁴²⁾、一酸化窒素合成酵素⁴³⁾をはじめとした、多くの Ca^{2+} 結合型カルモジュリン依存性酵素の活性を制御する。最近、 Ca^{2+} 結合型カルモジュリンがある種の癌細胞において異常に高発現していること⁴⁴⁾、 Ca^{2+} 結合型カルモジュリンの特異的アンタゴニストがさまざまな癌細胞の増殖を抑制すること⁴⁵⁾など、 Ca^{2+} 結合型カルモジュリンが癌細胞の増殖に重要な役割を果たしているという証拠が示されつつある。したがって、 Ca^{2+} 結合型カルモジュリンは癌の化学療法において有望な標的蛋白質であると認識されつつあり、筆者らの結果はこの可能性を支持するものである⁴⁶⁾。

■ おわりに

これまで述べたように、筆者らは、フォワード/リバースケミカルゲノミクスのアプローチを利用して、血管新生に関連する新しい低分子化合物と機能的な標的蛋白質を見いだしてきた(図7)。この強力な戦略は、血管新生以外の興味深い生物学的表現型にも応用が可能であり、遺伝子の機能的解析と医薬品の開発に新しい流れを提供するものである。

ケミカルゲノミクスは、化学と生物学におけるツールと技術を、蛋白質の機能解析と新しい医薬品の開発のために融合・利用することで出現してきた分野である。表現型の変化を指標に見いだされた天然低分子化合物や合

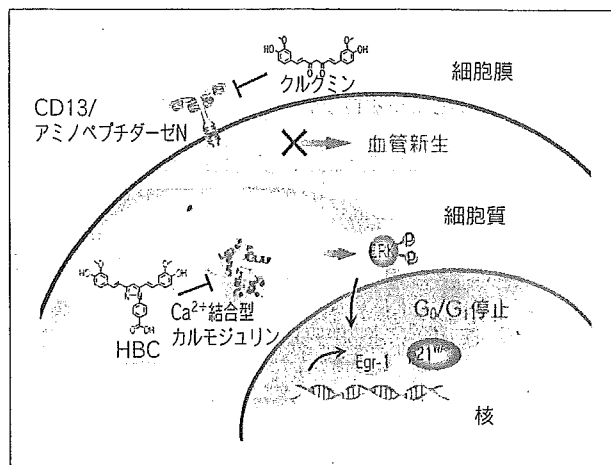


図7 筆者らが見いだした、血管新生に関連する新しい低分子化合物と、その標的蛋白質

成低分子化合物はケミカルゲノミクス研究に適している。本稿で示したように、この方法論は作用機構が不明な生理活性低分子化合物の標的蛋白質の同定に非常に有用である。このアプローチは、標的蛋白質同定のため全プロテオームおよび全ゲノムを利用するので、得られた結果は、より臨床に関連した蛋白質として応用が可能であり、医薬品開発にかかる時間を短縮し、かつ効率をあげることが可能である。また、ケミカルゲノミクスのアプローチは、医薬品開発にメリットがあるのみならず、未解明の生物機能の分子機構を探求するための重要な情報を提供する。フォワードケミカルゲノミクスにより得られたすべての新しい標的蛋白質は、化合物ライブラリーを利用したハイスループットスクリーニングや *in silico* スクリーニングによって、さらに強力な、かつ臨床開発が可能な医薬品の開発にも有用である。化学構造に基づいたドラッグデザインもまた、リバースケミカルゲノミクスの効率をよくする。このようなケミカルゲノミクスの学際的な様相は、複雑な生命科学を理解するための複数の異なる研究領域のかけ橋となるプラットフォームとしても非常に魅力的である。

J. S. Kim 博士の有益な助言に感謝する。

文献

- 1) Schreiber, S. L. : *Med. Chem.*, 6, 1127-1152 (1998).
- 2) Mitchison, T. J. : *Chem. Biol.*, 1, 3-6 (1994)
- 3) Crews, C. M., Splittgerber, U. : *Trends Biochem. Sci.*, 24, 317-320 (1999)

- 4) Stockwell, B. R. : *Nature Rev. Genet.*, 1, 116-125 (2000)
- 5) Kwon, H. J. : *Curr. Med. Chem.*, 10, 717-736 (2003)
- 6) De Luca, L. M. : *FASEB J.*, 5, 2924-2933 (1991)
- 7) Harding, M. W. *et al.* : *Nature*, 341, 758-760 (1989)
- 8) Lokey, R. S. : *Curr. Opin. Chem. Biol.*, 7, 91-96 (2003)
- 9) Sabers, C. J. *et al.* : *J. Biol. Chem.*, 270, 815-822 (1995)
- 10) Sin, N. *et al.* : *Proc. Natl. Acad. Sci. USA*, 94, 6099-6103 (1997)
- 11) Sche, P. P. *et al.* : *Chem. Biol.*, 6, 707-716 (1999)
- 12) Stockwell, B. R., Haggarty, S. J., Schreiber, S. L. : *Chem. Biol.*, 6, 71-83 (1999)
- 13) Horrocks, C. *et al.* : *Curr. Opin. Drug Discov. Dev.*, 6, 570-575 (2003)
- 14) Langer, T., Krovat, E. M. : *Curr. Opin. Drug Discov. Dev.*, 6, 370-376 (2003)
- 15) Folkman, J. : *Lab. Invest.*, 51, 601-604 (1984)
- 16) Folkman, J., Klagsbrun, M. : *Science*, 235, 442-447 (1987)
- 17) Folkman, J. : *Curr. Mol. Med.*, 3, 643-651 (2003)
- 18) Folkman, J. : *Adv. Cancer Res.*, 19, 331-358 (1974)
- 19) Moses, M. A., Langer, R. A. : *J. Cell Biochem.*, 47, 230-235 (1991)
- 20) Millauer, B. *et al.* : *Cell*, 72, 835-846 (1993)
- 21) Giles, F. J. *et al.* : *Cancer*, 97, 1920-1928 (2003)
- 22) Ingber, D. *et al.* : *Nature*, 348, 555-557 (1990)
- 23) Kwon, H. J. *et al.* : *Int. J. Cancer*, 97, 290-296 (2002)
- 24) Shim, J. S. *et al.* : *Bioorg. Med. Chem.*, 10, 2439-2444 (2002)
- 25) Oikawa, T. *et al.* : *Biochem. Biophys. Res. Commun.*, 181, 1070-1076 (1991)
- 26) Kelloff, G. J. *et al.* : *J. Cell Biochem.*, 26(suppl.), 54-71 (1996)
- 27) Aggarwal, B. B., Kumar, A., Bharti, A. C. : *Anticancer Res.*, 23, 363-398 (2003)
- 28) Huang, M. T. *et al.* : *Cancer Res.*, 54, 5841-5847 (1994)
- 29) Arbiser, J. L. *et al.* : *Mol. Med.*, 4, 376-383 (1998)
- 30) Folkman, J. : *J. Natl. Cancer Inst.*, 82, 4-6 (1989)
- 31) Burley, S. K. *et al.* : *J. Mol. Biol.*, 224, 113-140 (1992)
- 32) Luciani, N. *et al.* : *Biochemistry*, 37, 686-692 (1998)
- 33) Fujii, H. *et al.* : *Clin. Exp. Metastasis*, 13, 337-344 (1995)
- 34) Pasqualini, R. *et al.* : *Cancer Res.*, 60, 722-727 (2000)
- 35) Bhagwat, S. V. *et al.* : *Blood*, 97, 652-659 (2001)
- 36) Sche, P. P. *et al.* : *Chem. Biol.*, 6, 707-716 (1999)
- 37) Shim, J. S. *et al.* : *Chem. Biol.*, 11, 1455-1463 (2004)
- 38) Cheung, W. Y. : *Science*, 207, 19-27 (1980)
- 39) Walsh, M. P. *et al.* : *J. Biol. Chem.*, 254, 12136-12144 (1979)
- 40) Colbran, R. J., Soderling, T. R. : *Curr. Top. Cell. Regul.*, 31, 181-221 (1990)
- 41) Rybalkin, S. D., Bornfeldt, K. E. : *Thromb. Haemost.*, 82, 424-434 (1999)
- 42) Klee, C. B. : *Neurochem. Res.*, 16, 1059-1065 (1991)
- 43) Schmidt, H. H. *et al.* : *Cell Calcium*, 13, 427-434 (1992)
- 44) Wei, J. W., Morris, H. P., Hickie, R. A. : *Cancer Res.*, 42, 2571-2574 (1982)
- 45) Strobl, J. S., Peterson, V. A. : *J. Pharm. Exp. Ther.*, 263, 186-193 (1992)
- 46) Hait, W. N., Lazo, J. S. : *J. Clin. Oncol.*, 4, 994-1012 (1986)

Ho Jeong Kwon

略歴：1995年 東京大学大学院農学系研究科博士課程 修了，ハーバード大学 博士研究員を経て，1999年 Sejong 大学 准教授，2002年より同教授。 研究テーマ：ケミカルゲノミクス，ケミカルジェネティクス。

掛谷秀昭

略歴：1994年 慶應義塾大学大学院理工学研究科博士課程 修了，理化学研究所抗生物質研究室 研究員，マサチューセッツ工科大学 客員研究員を経て，2003年より理化学研究所中央研究所 長田抗生物質研究室 副主任研究員。 研究テーマ：天然物化学，ケミカルバイオロジー，ケミカルゲノミクス。

蛋白質 核酸 酵素

◆2004年2月号増刊を単行本化◆

神経回路の機能発現のメカニズム

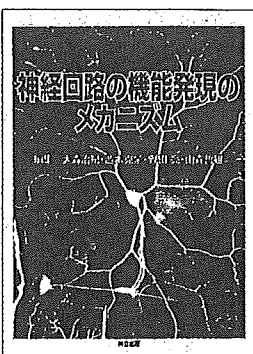
編集：大森治紀・澁木克栄・野田 亮・山森哲雄

CONTENTS

- | | |
|-------------------|--------------------|
| I. 神経細胞の分化と移動 | IV. シナプス可塑性と神経回路形成 |
| II. 受容体とシナプス形成 | V. 学習と行動の分子メカニズム |
| III. 神経回路形成の分子的基盤 | VI. 神経系の特徴抽出と統合機能 |

A4変型判・308頁・定価4,935円(税込)

共立出版



Phase I pharmacokinetic and pharmacogenomic study of E7070 administered once every 21 days

Yasuhide Yamada,^{1,3} Noboru Yamamoto,¹ Tatsu Shimoyama,¹ Atsushi Horiike,¹ Yasuhito Fujisaka,¹ Kyoko Takayama,¹ Terumi Sakamoto,¹ Yuki Nishioka,² Sanae Yasuda² and Tomohide Tamura¹

¹Medical Oncology Division, National Cancer Center Hospital, 5-1-1 Tsukiji, Chuo-ku, Tokyo 104-0045; and ²Clinical Research Center, Eisai Company, 4-6-10 Koishikawa, Bunkyo-ku, Tokyo 112-8088, Japan

(Received April 14, 2005/Revised July 12, 2005/Accepted July 29, 2005/Online publication October 3, 2005)

E7070 is a novel sulfonamide anticancer agent that disrupts the G₁/S phase of the cell cycle. The objectives of this phase I study of E7070 were to estimate the maximal tolerated dose (MTD), to determine the recommended dose for phase II, and to clarify the pharmacokinetic profile of E7070 and its relation to polymorphisms of CYP2C9 (*2, *3) and CYP2C19 (*2, *3) in Japanese patients. Patients received 1–2-h i.v. infusions of E7070 (400, 600, 700, 800 or 900 mg/m²) on day 1 of a 21-day cycle. Twenty-one patients received between one and eight cycles of E7070. The dose-limiting toxicities (DLT) comprised leukopenia, neutropenia, thrombocytopenia, elevation of aspartate aminotransferase, colitis, and ileus. The mean area under the plasma concentration–time curve (AUC) for successive dose levels increased in a non-dose-proportional manner. Two patients were heterozygous for the CYP2C9 mutation. For CYP2C19, eight patients were wild type and the remainder had heterozygous (*n* = 8) or homozygous mutations (*n* = 5). Regarding the CYP2C19 genotype, the AUC of patients with mutant alleles were higher than those of patients with wild type at a dose of 600 mg/m² or more. The severity of toxic effects, such as myelosuppression, seemed to depend on the AUC. No partial responses were observed. One patient treated at a dose of 700 mg/m² experienced a maximum tumor volume reduction of 22.5%. The MTD was estimated to be 900 mg/m². A dose of 800 mg/m² is recommended for further phase II studies. The pharmacokinetic/pharmacodynamic properties of E7070 seemed to be influenced by CYP2C19 genotype. The observed safety profile and preliminary evidence of antitumor activity warrant further investigation of this drug in monotherapy or in combination chemotherapy. (*Cancer Sci* 2005; 96: 721–728)

E7070, *N*-(3-chloro-7-indolyl)-1,4-benzenedisulfonamide, has been reported to exhibit a potent antitumor activity by blocking cell cycle progression. *In vitro* studies indicate that the drug disrupts the G₁/S phase, thereby inducing cell cycle arrest and apoptosis.⁽¹⁾ Although E7070 is not a direct inhibitor of cyclin-dependent kinases (CDK), it causes depletion of cyclin E, with a reduction in CDK2 catalytic activity.⁽²⁾ The exact mechanism of cyclin E/CDK2 inactivation is unclear. Transcriptional repression of cyclin H in a p53-independent manner also occurs in response to E7070.⁽³⁾ The reduction in G₁ CDK activity induces arrest at the G₁/S boundary, accompanied by hypophosphorylation of retinoblastoma (Rb) protein and decreases in CDK2, cyclin A, and cyclin B proteins.⁽¹⁾ E7070 activity is associated with upregulation of p53 and p21, which may contribute to the

reduced Rb phosphorylation, as well as subsequent apoptosis. In preclinical models, E7070 was cytotoxic to human HCT116 colon carcinoma and LX-1. E7070 exhibits more potent *in vivo* antitumor effects than 5-fluorouracil, mitomycin C, and irinotecan.⁽⁴⁾

E7070 has been the subject of four clinical phase I studies. In the first trial, E7070 was administered once every 21 days at doses between 50 and 1000 mg/m²,⁽⁵⁾ and in the second trial E7070 was administered five times per day once every 3 weeks at doses between 10 and 200 mg/m² per day.⁽⁶⁾ Other schedules used were a weekly infusion given over 4 consecutive weeks repeated every 6 weeks,⁽⁷⁾ and a continuous intravenous infusion for 5 days every 3 weeks.⁽⁸⁾ In the single-dose every 3 weeks study, neutropenia and thrombocytopenia were dose-limiting at 700 and 800 mg/m².⁽⁵⁾ In the second study, neutropenia and thrombocytopenia were dose-limiting at 160 and 200 mg/m².⁽⁶⁾ In the study that used a weekly dose schedule, neutropenia and thrombocytopenia were also dose-limiting toxicities (DLT) and other DLT included stomatitis, diarrhea, nausea, and fatigue.⁽⁷⁾ Partial responses were observed in patients with breast and endometrial cancer.^(6,7)

During a phase I trial, three patients receiving prophylactic daily oral maintenance therapy with acenocoumarol developed a hemorrhagic tendency and/or a prolonged prothrombin time following treatment with 700 and 800 mg/m² of E7070.⁽⁵⁾ The major metabolic enzyme for acenocoumarol is cytochrome P450 (CYP)2C9.⁽⁹⁾ *In vitro* studies have shown that E7070 has the potential to inhibit CYP2C9 and CYP2C19.⁽¹⁰⁾ The pharmacokinetic drug–drug interaction study indicated that primary interaction of the two drugs could occur via inhibition by E7070 of acenocoumarol metabolism.

Based on these results from the previous phase I and pharmacokinetic trials, the present phase I study was designed to evaluate ascending doses of E7070 administered as a single dose by 1–2-h i.v. infusion every 21 days. The objectives of the study were to determine the maximum tolerated dose (MTD) and the dose to be recommended for use in future phase II studies, as well as to assess the safety, pharmacokinetic profile and preliminary antitumor activity of the drug. We also evaluated the influence of genetic polymorphisms of CYP2C9 and CYP2C19 on the pharmacokinetics of E7070.

³To whom correspondence should be addressed. E-mail: yayamada@ncc.go.jp

Materials and Methods

Patient selection

Japanese patients with histologically or cytologically confirmed malignant solid tumors refractory to conventional chemotherapy, or tumors for which no effective therapy was available, were candidates for this study. Eligibility criteria included the following: age between 20 and 75 years; World Health Organization (WHO) performance status 0–1, life expectancy ≥ 3 months, absolute leukocyte count $\geq 4000/\mu\text{L}$ and $< 12\,000/\mu\text{L}$, absolute neutrophil count $\geq 2000/\mu\text{L}$, hemoglobin level $\geq 9\text{ g/dL}$, platelet count $\geq 100\,000/\mu\text{L}$, serum creatinine level $< 1.5\text{ mg/dL}$ or creatinine clearance $\geq 50\text{ mL/min}$, and arterial partial pressure of oxygen of 65 torr or more. Additional entry criteria were serum bilirubin $\leq 1.5\text{ mg/dL}$, and serum aspartate aminotransferase (AST) and alanine aminotransferase (ALT) $\leq 100\text{ IU/L}$. Before study entry, a 6-week interval was required for patients previously treated with mitomycin C or nitrosoureas, a 4-week interval was required for other chemotherapy, endocrinotherapy, surgery, radiation therapy, immunotherapy treatments or other investigational agents, and a 2-week interval after blood transfusion or administration of granulocyte-colony stimulating factor (G-CSF). Patients were ineligible for the study if they had symptomatic central nervous system metastases, active infection, or other non-malignant disease, which was considered to be incompatible with the protocol. Patients who were receiving corticosteroids or coumarin anticoagulants less than 2 weeks prior to administration of E7070 were excluded from the study. The protocol was approved by the institutional review boards of the National Cancer Center, and all patients gave written informed consent prior to study entry.

Dosage and dose escalation

E7070 was provided as a lyophilized powder in 500-mg vials by Eisai Co. (Tokyo, Japan). The starting dose of E7070 was set at 400 mg/m^2 because only mild to moderate grade 1 to grade 2 toxicity was observed at doses of 600 mg/m^2 or lower in the previous phase I study.⁽⁶⁾ Subsequent doses were to be escalated to 600, 700, 800 and 900 mg/m^2 . E7070 was dissolved in 20 mL of distilled water, then added to 500 mL of normal saline for injection, and this solution was administered by intravenous infusion over 1 h at doses of 400 and 600 mg/m^2 . Injection site reaction was observed in one of three patients at 400 mg/m^2 and three of three patients at 600 mg/m^2 . Therefore, E7070 was given in 1000 mL of normal saline over 2 h at 700, 800, and 900 mg/m^2 . Patients were hospitalized for the first course of E7070 and remained hospitalized for close observation for 21 days thereafter. Subsequent courses could be administered on an outpatient basis with weekly patient evaluations by the investigator.

Patients were enrolled in cohorts of three patients per dose level and observed for 21 days; the observation period was extended to 42 days if a longer recovery period was needed. If one of the three patients experienced DLT, then three additional patients were treated at the same dose. If two or more of three or six patients experienced DLT, that dose level was regarded as the MTD. If none of the first three patients demonstrated DLT, then the next three patients were treated at the

next (higher) dose level. Individual patients who did not demonstrate DLT and showed no evidence of disease progression could receive E7070 at the originally assigned dose.

After the MTD had been determined, a dose below the MTD was evaluated in a total of six patients for identification of the proposed recommended dose for phase II study. The recommended dose was the highest dose at which less than 33.3% of treated patients experienced DLT.

Definition of dose-limiting toxicity

The DLT was defined as the occurrence of any of the following events during cycle 1 that were attributable to E7070: National Cancer Institute Common Toxicity Criteria (NCI CTC) (version 2.0) grade 3 or 4 non-hematological toxicity (except nausea, vomiting effectively managed with symptomatic treatment, or alopecia), grade 4 leukopenia, grade 4 neutropenia accompanied by fever of $\geq 38.5^\circ\text{C}$, or that persisted ≥ 5 days, and platelet count $< 25\,000/\mu\text{L}$. Prophylactic use of colony-stimulating factors was not permitted during the first cycle; however, patients who had neutropenia that had met the criteria for DLT were permitted to receive concomitant treatment with G-CSF.

Evaluation of patients

Safety was evaluated on the basis of physical findings, vital signs, adverse events, and laboratory parameters obtained at baseline and periodically throughout the study. During the first cycle, hematology studies were performed at least twice a week, while vital signs, physical examinations (including evaluation of performance status) and serum biochemistry were measured on days 1, 8 and 15. Toxicity evaluations of subjective and objective findings were performed according to the NCI CTC (version 2.0) on days 1, 8 and 15. For the second and subsequent cycles, vital signs, laboratory tests and toxicity evaluations based on subjective and objective findings were performed on days 1, 8, and 15 of each cycle. Blood glucose was monitored before the dose of E7070 and after the end of infusion. Blood coagulation studies were carried out before each dose for all cycles and also at day 8 of the first cycle. Efficacy was assessed by the physician on the basis of antitumor effect according to the Response Evaluation Criteria in Solid Tumors (RECIST).⁽¹¹⁾ If an antitumor effect was observed, the disease site was re-evaluated at least 4 weeks later to confirm the response.

Pharmacokinetics

Pharmacokinetic studies were performed during the first cycle of treatment. On day 1, blood samples (4 mL each) were drawn from an indwelling intravenous cannula in the arm contralateral to that bearing the infusion line. Samples were collected in heparinized tubes, preinfusion, at 30 min after the start of the infusion, at the end of the 1- or 2-h infusion, and at 10, 30, and 60 min and 2, 4, 6, 10, 24, 48, 72, 96, 168, and 240 h after the infusion. The samples were centrifuged at $1500\times g$ for 10 min at 5°C , and the resulting plasma samples were stored at -20°C until analysis. Urine samples were collected before the start of E7070 infusion and over three 24-h intervals for 72 h after the start of the infusion. The concentrations of E7070 in plasma and in urine were analyzed at Eisai Co. by means of validated high-performance

liquid chromatography methods with UV detection (HPLC-UV). The lower limit of quantification was 20 ng/mL. *N*-(3-Chloro-7-indolyl)-4-(*N*-methylsulfamoyl)benzenesulfonamide (ER-67771)⁽¹²⁾ was used as an internal standard.

Plasma, the internal standard and 0.1 mol/L phosphate buffer (pH 6.8) were vortexed. After adding ethyl acetate, the mixture was shaken and centrifuged. The organic layer was collected and transferred into a glass tube, then evaporated under nitrogen flow in a drying block. The residue was dissolved in CH₃CN-6.7 mmol/L phosphate buffer (pH 6.6), and the solution was injected into an HPLC apparatus.

Chromatographic separation was achieved by using a column switching method with Asahipak C8P-50 (Showa Denko, Tokyo, Japan) as a separation column and YMC-pack ODS-AM-312 (YMC) as an analytical column. Mobile phases were CH₃CN: 6.7 mmol/L phosphate buffer (pH 6.6; 360:640 [v:v]) for separation and CH₃CN: 6.7 mmol/L phosphate buffer (pH 7.4; 360:640 [v:v]) for analysis. E7070 was monitored by UV detection at 280 nm.

Pharmacokinetic parameters of E7070 after a single dose administration during the first cycle were determined by non-compartmental analysis using WinNONLIN (Pharsight Corporation, CA, USA). The apparent elimination rate constant at the terminal phase (λ_z) was estimated by linear regression analysis from the terminal log-linear declining phase to the last quantifiable concentration. The elimination half-life ($t_{1/2}$) was calculated as $t_{1/2} = \ln(2)/\lambda_z$. The area under the plasma concentration-time curve from zero to the last quantifiable sampling time, $AUC_{(0-t_n)}$, was obtained by the log trapezoidal rule. The AUC from zero to infinity was calculated as $AUC_{(0-t_n)} + C_n/\lambda_z$, where C_n was the last quantifiable concentration. The clearance was calculated as dose/AUC. The mean residence time (MRT) was estimated from $AUMC/AUC$, where AUMC is the first moment curve. The volume of distribution was calculated as $MRT \times \text{clearance}$.

Genotyping procedures for CYP2C9 and CYP2C19

Genotyping was conducted using the Invader assay (BML, Tokyo, Japan). Genomic DNA was isolated from whole blood with the QIAamp DNA Blood Kit (Qiagen, CA, USA). The primary probes (wild type and mutant probes) were used to detect C430T (*2) and A1075C (*3) mutations of CYP2C9, and G681A (*2) and G636A (*3) of CYP2C19, respectively. The invader assay fluorescent resonance energy transfer (FRET)-detection 96-well plates (Third Wave Technologies, WI, USA) contained Cleavase enzyme, FRET probes, MOPS buffer and polyethylene glycol. Eight microliters of mixtures consisting of an appropriate primary probe, Invader oligonucleotide and MgCl₂ was added to the wells, followed by addition of 7 μ L of the heat-denatured genomic DNA, and this was overlaid with 15 μ L of mineral oil. For only CYP2C9*2 (C430T) detection, a dilution of the CYP2C9-specific polymerase chain reaction (PCR) product was used instead of genomic DNA, because the CYP2C9*2 (C430T) detection point has the same sequence on CYP2C19. The plates were incubated at 63°C for 4 h for genomic DNA or 1 h for the PCR product. The fluorescence intensities were measured on a Cytofluor 4000 fluorescence plate reader (Applied Biosystems, CA, USA) with excitation at 485/20 nm (wavelength/bandwidth) and emission at 530/

Table 1. Patients' characteristics

No. entered	21
Age (years)	
Median	57
Range	35-70
Male:female (no. patients)	15:6
WHO performance status (no. patients)	
0	7
1	14
Tumor type (no. of patients)	
Colorectal	15
SCLC	2
Gastric	1
NSCLC	1
Liposarcoma	1
Mesothelioma	1
Prior treatment	
Chemotherapy	
No. prior regimens (no. patients)	
0	0
1	1
2	5
>3	15
Surgery (no. patients)	18
Radiation therapy (no. patients)	7

SCLC, small cell lung cancer; NSCLC, non-small cell lung cancer; WHO, World Health Organization.

25 nm for FAM dye detection, and excitation at 560/20 nm and emission at 620/40 nm for RED dye detection.

Subjects having either the *2 or *3 allele (*1/*2 or *1/*3) were defined as hetero extensive metabolizers (hetero EM), those with two mutated alleles (*2/*2, *2/*3 or *3/*3) as poor metabolizers (PM), and those with no mutated alleles (*1/*1) as homo EM.

Results

Patients' characteristics

Twenty-one patients (15 male and six female) were enrolled into the study (Table 1). All patients had a good performance status and had received previous chemotherapy regimens. The colon/rectum was the most commonly noted primary disease site. All patients were evaluable for toxicity during the first cycle, and for efficacy. Twenty-one patients received 42 cycles of treatment. The median number of cycles administered per patient was one (range, 1-8).

Dose escalation and identification of DLT, MTD, and the recommended phase II dose

The DLT in this study were leukopenia, neutropenia, thrombocytopenia, elevation of AST, colitis, and ileus. None of the patients treated at any dose of less than 800 mg/m² experienced DLT. At a dose of 900 mg/m², two of three patients experienced dose-limiting leukopenia, neutropenia, and thrombocytopenia, identifying this dose level as the MTD. At the same dose, grade 3 colitis and grade 3 AST elevation were observed in one patient. Therefore, three additional patients were enrolled at 800 mg/m². One of the additional three patients evaluated for safety at 800 mg/m² experienced

Table 2. Hematological toxicities during the first cycle of treatment with E7070

Toxicity	Grade	Dose (mg/m ²)				
		400 (n = 3)	600 (n = 3)	700 (n = 6)	800 (n = 6)	900 (n = 3)
Neutropenia	1/2	0	0	3	1	0
	3/4	0	2	0	3	3
Leukopenia	1/2	1	2	3	3	1
	3/4	0	0	0	2	2
Thrombocytopenia	1/2	0	2	1	2	0
	3/4	0	0	0	1	3
Anemia	1/2	1	2	4	2	2
	3/4	0	0	0	1	1

DLT of grade 3 ileus. This patient had previously undergone intestinal surgery for colon cancer. On the basis of these findings, a total of six patients were treated at the dose of 800 mg/m² and one of the six patients experienced DLT. Thus, based on protocol-defined criteria, the MTD was estimated to be 900 mg/m². Therefore, a dose of 800 mg/m² is the recommended dose for single-agent phase II studies.

Hematological toxicity

Neutropenia, leukopenia, and thrombocytopenia were the hematological toxicities observed most commonly during the first cycle (Table 2). Neutropenia was the principal hematological toxicity in this study and was dose-limiting at 900 mg/m². Eight patients treated at 600, 800 and 900 mg/m² experienced grade 3 or more neutropenia. In these patients the median times to nadir neutrophil counts were 12.5 (8–25) days in the first cycle and 15.5 (8–25) days in all cycles, and the median times to recovery from nadir to grade 1 were 5.0 (3–15) days in the first cycle and 6.0 (3–15) days in all cycles. Neutrophil counts recovered to grade 1 within 21 days after E7070 infusion in all patients treated with 400 mg/m², but had not recovered by day 22 in two, one and two patients at 600, 700 and 800 mg/m², respectively. Neutrophil counts recovered by day 29 after E7070 infusion in all patients. G-CSF support was provided during cycle 1 in two of three patients treated at 900 mg/m². One patient treated at 800 mg/m² and three patients treated at 900 mg/m² experienced grade 3 thrombocytopenia. In patients treated at 800 and 900 mg/m², the median time to nadir platelet counts was 10.0 (7–12) days, and the median time to recovery from nadir to grade 1 was 5.0 (2–9) days in the first cycle. Anemia, reported in 13 (62%) patients, did not exceed grade 1–2 severity except in two patients at 800 and 900 mg/m². The numbers of patients with blood cell count toxicity did not tend to increase with increasing number of courses of treatment, suggesting that the hematological toxicity of E7070 is not cumulative.

Non-hematological toxicity

The non-hematological toxicities reported commonly during the first cycle were rash, fatigue, stomatitis, alopecia, injection site reaction, diarrhea and constipation (Table 3). These toxicities were generally mild. Grade 3 and grade 4 toxicities were reported in patients treated with 800 or 900 mg/m². Grade 3 ileus and grade 4 constipation associated with the

ileus developed in one patient at 800 mg/m². Grade 3 AST elevation, grade 3 colitis and grade 3 diarrhea accompanying the colitis were observed in one patient at 900 mg/m². The toxicities reported most commonly in subsequent cycles were similar in terms of number of patients affected and severity to those reported during the first cycle of treatment.

Gastrointestinal toxicity, usually mild, was the most common non-hematological toxicity associated with E7070. Diarrhea (grades 1–3) was noted in eight (38%) patients during the first cycle, and the incidence was greater at the 800 mg/m² (5/6) and 900 mg/m² (3/3) doses than at the 400–600 mg/m² doses (none). Severe diarrhea (grade 3) was observed in only one patient, who received 900 mg/m² and had previously undergone surgery for primary colorectal cancer. In almost all cases, nausea and vomiting responded well to antiemetic therapies and patients were able to maintain good oral intake. Mild constipation (grades 1–2) was noted at 600–900 mg/m², except for one patient with grade 4 constipation associated with grade 3 ileus at 800 mg/m². Alopecia was observed in nine (43%) patients. Grades 1–2 injection site reaction, including irritation, pain, or phlebitis, developed in one patient at 400 mg/m² and three patients at 600 mg/m². Therefore, E7070 in 1000 mL of normal saline was given over 2 h at 700, 800, and 900 mg/m². However, three patients at 700 mg/m² and two patients at 800 mg/m² showed injection site reaction, and thus E7070 was given to patients at 900 mg/m² through a central vein. There were no deaths within 28 days of E7070 administration, and none of the deaths that occurred after the study was considered to have been treatment-related.

Pharmacokinetics

Complete pharmacokinetic data sets were obtained in 21 patients. The mean (+SD) plasma concentration-time curves of E7070 are shown in Figure 1. The mean (± SD) pharmacokinetic parameters derived from the plasma concentration are listed in Table 4. After the end of the infusion, plasma concentration of E7070 decreased rapidly for several hours, followed by a slower elimination phase (Fig. 1). During the elimination phase, the E7070 plasma concentration-time profile was convex, which is characteristic of non-linear pharmacokinetics. Maximum plasma concentrations (C_{max}) of E7070 at the 700–900 mg/m² doses were lower than that at 600 mg/m² (Table 4). This is probably related to the change of the infusion time of E7070 from 1 h to 2 h at doses over

Table 3. Non-hematological toxicities during the first cycle of treatment with E7070

Toxicity	Grade	Dose (mg/m ²)				
		400 (n = 3)	600 (n = 3)	700 (n = 6)	800 (n = 6)	900 (n = 3)
Diarrhea	1/2	0	0	0	5	2
	3	0	0	0	0	1
Constipation	1/2	0	1	2	3	1
	3/4	0	0	0	1	0
Nausea	1/2	0	1	3	1	1
	3	0	0	0	1	0
Vomiting	1/2	0	1	0	0	0
	3	0	0	0	1	0
Anorexia	1/2	0	1	2	1	1
	3	0	0	0	1	0
Stomatitis	1/2	1	1	2	3	3
	3	0	0	0	0	0
Injection site reaction	1/2	1	3	3	2	0*
	3	0	0	0	0	0*
Rash	1/2	1	1	5	2	3
	3	0	0	0	0	0
Fatigue	1/2	1	2	2	3	3
	3	0	0	0	0	0
Headache	1/2	1	1	4	2	0
	3	0	0	0	0	0
Alopecia	1/2	0	1	2	3	3

*E7070 was administered through a central vein at a dose of 900 mg/m².

Table 4. Pharmacokinetic parameters of E7070

Dose (mg/m ²)	No. patients	C _{max} (µg/mL)	AUC (µg·h/mL)	CL (mL/min per m ²)	MRT (h)	t _{1/2} (h)	V _{ss} (L/m ²)	Urinary excretion (%)
400	3	82.2 ± 15.4	1066 ± 140	6.3 ± 0.9	26 ± 8	20 ± 5	9.8 ± 1.6	0.82 ± 0.22
600	3	142.8 ± 12.3	4204 ± 1353	2.6 ± 1.0	53 ± 17	32 ± 11	7.6 ± 0.0	1.67 ± 0.13
700	6	116.1 ± 11.3	3300 ± 1058	3.9 ± 1.3	41 ± 12	21 ± 7	8.7 ± 0.9	1.57 ± 0.39
800	6	117.7 ± 8.6	3943 ± 1243	3.6 ± 1.0	45 ± 11	22 ± 4	9.2 ± 0.8	1.77 ± 0.80
900	3	133.8 ± 0.7	6095 ± 1009	2.5 ± 0.4	59 ± 10	27 ± 8	8.7 ± 0.7	2.47 ± 1.33

C_{max}, maximum plasma concentration; AUC, area under the plasma concentration-time curve; CL, clearance; MRT, mean residence time; t_{1/2}, terminal elimination half-life; V_{ss}, distribution volume at steady state; urinary excretion, cumulative excreted amount of E7070 in urine.

600 mg/m² because of injection site reaction. The AUC increased more than expected with increasing dose. The clearance decreased between 400 and 900 mg/m², with mean values of 6.3 mL/min per m² to 2.5 mL/min per m². The mean plasma half-life (t_{1/2}) was between 20 and 32 h at the examined doses. Mean 72-h urinary excretion was 0.82% to 2.47% of the administered dose of E7070 in the five cohorts.

Pharmacodynamics

The pharmacodynamic analysis was performed by focusing on leukopenia, neutropenia and thrombocytopenia, because these were the DLT of E7070. Figure 2 shows that the nadirs of white blood cells (WBC), neutrophils, and platelets were related to the AUC of E7070. The percentage decrease rate from the value before dosing to the nadir of WBC, neutrophil or platelet count also showed a good correlation with the AUC of E7070.

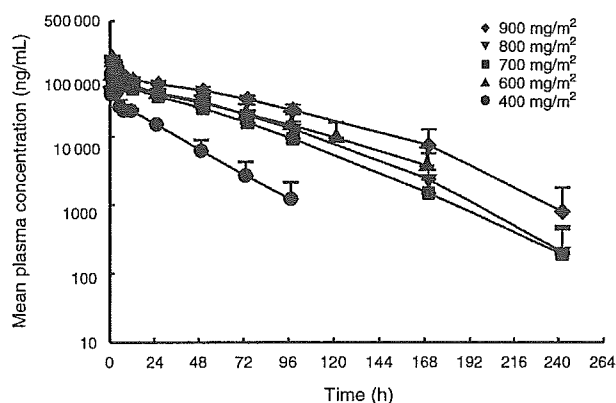


Fig. 1. Mean plasma concentrations of E7070 after single intravenous infusion at each dose level. Circles, 400 mg/m²; triangles, 600 mg/m²; squares, 700 mg/m²; inverted triangles, 800 mg/m²; diamonds, 900 mg/m². Each point represents the mean with standard deviation.

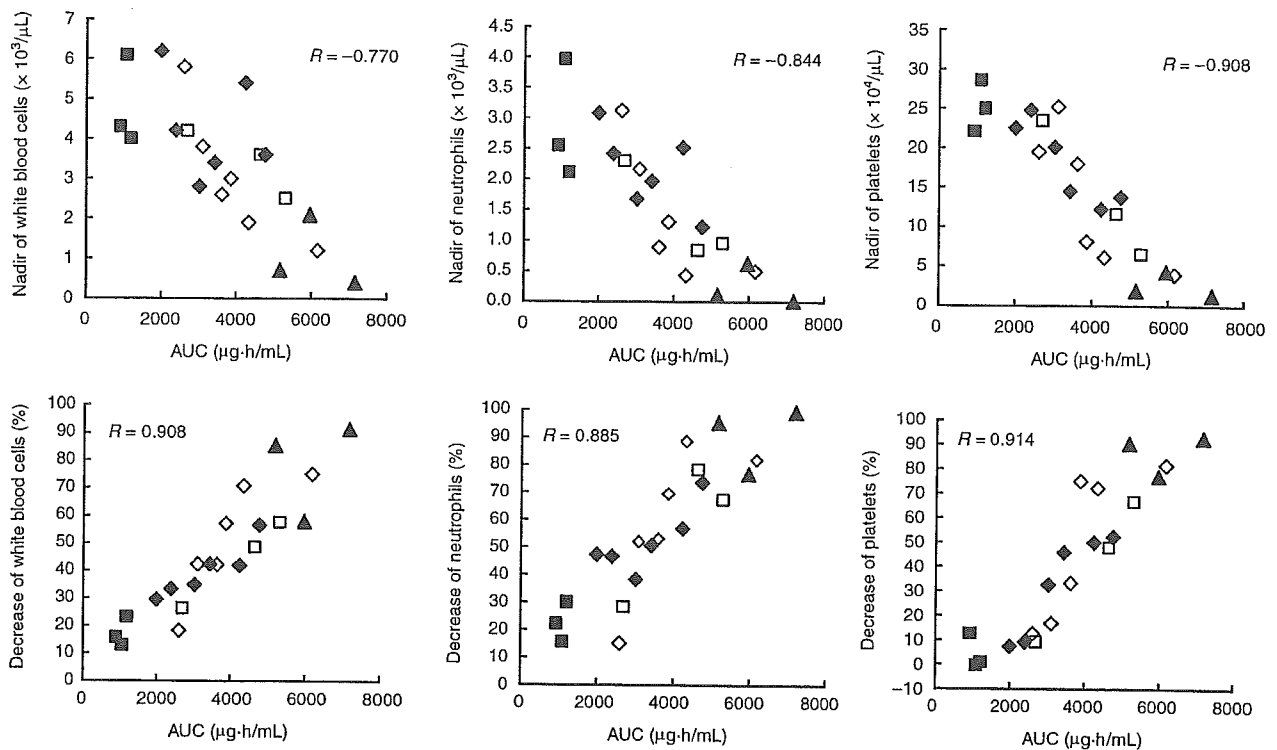


Fig. 2. Relationship between the area under the plasma concentration–time curve (AUC) of E7070 and white blood cells, neutrophil and platelet counts. Closed squares, 400 mg/m²; open squares, 600 mg/m²; closed diamonds, 700 mg/m²; open diamonds, 800 mg/m²; closed triangles, 900 mg/m². R, Pearson's correlation coefficient.

Genotyping of CYP2C9 and CYP2C19

The CYP2C9 and CYP2C19 genotypes were studied in 21 patients. Two (10%) were hetero EM for CYP2C9 (*1/*3), and 19 (90%) were homo EM for CYP2C9 (*1/*1). Five (24%) were PM for CYP2C19 (*2/*2 or *2/*3), eight (38%) were hetero EM for CYP2C19 (*1/*2 or *1/*3) and eight (38%) were homo EM for CYP2C19 (*1/*1). Figure 3 shows the relationship between dose and AUC of E7070 with respect to CYP2C9 and CYP2C19 genotypes. At a dose level of 600 mg/m² or more, the AUC of patients with mutant allele(s) (PM and hetero EM) of CYP2C9 or CYP2C19 were higher than those of the patients without mutant alleles (homo EM). DLT was observed in one CYP2C19 PM patient at 800 mg/m² and two CYP2C19 hetero EM or PM patients at 900 mg/m².

Antitumor activity

No objective clinical responses were observed, but liver metastasis was reduced by 22.5% at the 8th cycle of 700 mg/m² in one colorectal cancer patient, who had previously received 5-fluorouracil.

Discussion

This phase I study was conducted to determine the MTD of E7070 administered by intravenous infusion over 1–2 h every 21 days, to determine the recommended single-agent dose for phase II studies, and to characterize the safety, pharmacokinetic and pharmacodynamic profiles of E7070. The

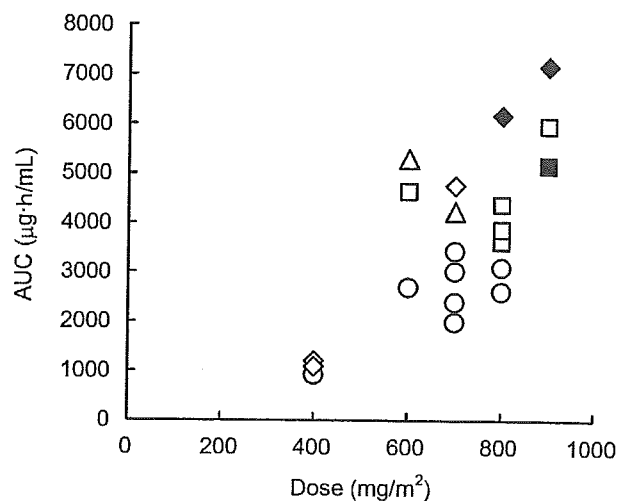


Fig. 3. Relationship between dose and area under the plasma concentration–time curve (AUC) of E7070 in relation to CYP2C9 and CYP2C19 genotypes. Circles, homo extensive metabolizers (EM) for both CYP2C9 and CYP2C19; squares, homo EM for CYP2C9 and hetero EM for CYP2C19; triangles, hetero EM for both CYP2C9 and CYP2C19; diamonds, homo EM for CYP2C9 and poor metabolizers (PM) for CYP2C19. Patients with dose-limiting toxicity are indicated with closed symbols.

MTD in this study was estimated to be 900 mg/m², and the recommended dose for phase II studies is 800 mg/m². DLT observed at 900 mg/m² included leukopenia, neutropenia, thrombocytopenia, elevation of AST, and colitis.

The hematological abnormalities most commonly reported during the first cycle of treatment were neutropenia, leukopenia, and thrombocytopenia. Neutropenia, which tended to be dose-dependent, but not course-dependent, was the principal hematological toxicity in this study and was dose-limiting at 900 mg/m². At the recommended dose of 800 mg/m², the mean recovery time of neutrophils from day 1 to grade 1 neutropenia was 24.0 ± 6.1 days. Therefore, bone marrow recovery should be confirmed before the start of successive treatment cycles. Hematological toxicities were also dose-limiting in four previous phase I trials of E7070.⁽⁵⁻⁸⁾

The non-hematological toxicities most commonly reported during the first cycle of treatment were rash, fatigue, stomatitis, alopecia, injection site reaction, diarrhea and constipation. The type and incidence of the frequently noted events were generally consistent across dosages and cycles of treatment. Gastrointestinal toxicity, the most common non-hematological type of toxicity associated with E7070, was usually mild and well-controlled with medication. The frequency of diarrhea increased with dose, and grade 3 severe diarrhea and colitis were observed only in one patient at 900 mg/m²; this patient had previously undergone intestinal surgery for colon cancer. Diarrhea was a dose-limiting toxicity in two previous phase I trials of E7070.^(6,7) Because of the relatively high frequency and dose-dependency of diarrhea in this study, patients receiving E7070 should be carefully monitored for diarrhea. Grade 3 ileus followed by grade 4 constipation was reported in one patient treated with 800 mg/m² of E7070. Although this event appeared to be related to peritoneal dissemination, its onset after 7 days of E7070 infusion suggested that it might have been induced by E7070. None of the patients treated at less than 800 mg/m² had grade 2 or higher nausea, vomiting, or anorexia.

Grades 1-2 rash, commonly localized to the face, anterior chest, and upper back, with mild itching, was observed in 12 patients given 400-900 mg/m² of E7070. Its frequency and severity were not dose-dependent. Rashes recovered within a week after the administration of E7070, and skin toxicity did not interrupt the therapy in any patient. Injection site reaction (grades 1-2) was reported in nine (43%) patients. The frequency of this event did not seem to be dose-dependent, suggesting that it was related to infusion irritation by E7070, rather than hemolysis or thrombosis. E7070 shows similarities to chloroquineoxaline sulfonamide, which is known to cause hypoglycemia and cardiac tachycardia.⁽¹³⁾ However, no hypoglycemia or cardiac arrhythmia was observed in this phase I trial of E7070.

The results of pharmacokinetic analysis suggested that the AUC of E7070 was non-linearly related to dose within the dose range of 400-900 mg/m². The clearance seemed to decrease, with a disproportionate increase in AUC. These results were in agreement with those obtained in other phase I trials with Caucasian patients.⁽⁵⁻⁸⁾ This non-linearity was prominent at higher dose levels and is likely to be a complex consequence of saturation of metabolism, protein binding and distribution of E7070.⁽¹⁴⁾ The absolute values of nadirs and the decrease ratios of WBC, neutrophil and platelet

counts were apparently correlated with the AUC of E7070. *In vitro* experiments have shown that E7070 has the potential to inhibit CYP2C9 and CYP2C19, suggesting that these CYP may be involved in the metabolism of E7070.⁽¹⁰⁾ In fact, other *in vitro* experiments have shown that CYP2C9 and CYP2C19 are responsible for the metabolism of E7070 (unpublished data). Since these CYP show genetic polymorphism, there is a possibility that subjects with one or more mutant alleles of these CYP have decreased clearance for any compound that is mainly metabolized by these polymorphic CYP. Therefore, we were prompted to investigate the relationship of the pharmacokinetics of E7070 with CYP2C9 and CYP2C19 genotype in this trial. At a dose level of 600 mg/m² or more, the AUC of patients with mutant allele(s) (PM and hetero EM) of CYP2C19 were higher than those of the patients without mutant alleles (homo EM). These results imply that the presence of mutant allele(s) of CYP2C19 may result in a decrease in the clearance of E7070 (Fig. 3), and support the involvement of CYP2C19 in the metabolism of E7070, as suggested from *in vitro* studies. The difference of AUC between CYP2C19 homo EM and PM was not clear at a dose of 400 mg/m². This was probably because metabolic capacity was less saturated at the low dose of 400 mg/m² compared with the higher doses, and so intergenotypic differences did not appear. The influence of the CYP2C9 genotype on the AUC of E7070 was not clarified because only two subjects had a mutant allele of this gene. The incidence of CYP2C9 PM is known to be less in Asian (< 1%) than in Caucasian (< 10%) people,^(15,16) whereas CYP2C19 PM is more frequent in Asian (20%) than in Caucasian (< 1%) people.⁽¹⁷⁾ Due to the low frequency of mutation of CYP2C9 in Asian populations, investigation of the effect of CYP2C9 on the pharmacokinetics of E7070 might be difficult in Japanese subjects. Research on subjects with various racial origins would be necessary for evaluation of the clinical impact of the CYP2C9 genotype. In any case, because of the small number of subjects in the present study, further studies should be taken into consideration to assess whether either the CYP2C9 or CYP2C19 genotype is of any clinical significance from the viewpoints of safety and efficacy of E7070. Urinary excretion of unchanged E7070, up to 72 h after the start of administration, was only 0.82-2.47% of the administered dose, indicating that renal clearance plays only a minor role in the elimination of E7070.

Although clinical efficacy (in terms of confirmed partial or complete responses) of E7070 was not demonstrated in this study, one patient with liver metastasis from colon cancer had a reduction in tumor size of ≤ 22.5% and demonstrated stable disease lasting 5 months. A phase II trial of E7070 as a single agent in 5-fluorouracil-resistant or refractory colorectal cancer showed limited activity with a 4% response rate,⁽¹⁸⁾ and thus further clinical studies of combination therapy with irinotecan (CPT-11) are ongoing for the treatment of this tumor type.

In conclusion, the MTD of E7070 administered intravenously in a 1-2 h infusion every 3 weeks was estimated to be 900 mg/m² and the recommended dose for a phase II study is 800 mg/m². At 800 mg/m², hematological toxicities were manageable. Gastrointestinal toxicity was the most common non-hematological toxicity associated with E7070, but was generally well controlled with premedication. However, this recommended dose might be influenced by the CYP2C19

genotype and possibly by the CYP2C9 genotype as well. E7070 seems to be an interesting agent with novel cell-cycle-inhibitory effects. Additional phase I and II studies are currently ongoing in various tumor types to explore further the antitumor activity of this drug as a single agent and in combination with other chemotherapeutic agents.

References

- 1 Fukuoka K, Usuda J, Iwamoto Y *et al.* Mechanism of action of the novel sulfonamide anticancer agent E7070 on cell cycle progression in human non-small cell lung cancer cells. *Invest New Drugs* 2001; **19**: 219–27.
- 2 Sugi N, Ozawa Y, Watanabe T *et al.* A novel agent ER-35744, targeting G1 phase. II: Antitumor activities *in vitro* and *in vivo*. *Proc Am Assoc Cancer Res* 1996; **37**: A2668.
- 3 Yokoi A, Kuromitsu J, Kawai T *et al.* Profiling novel sulfonamide antitumor agents with cell-based phenotypic screens and array-based gene expression analysis. *Mol Cancer Ther* 2002; **1**: 275–86.
- 4 Ozawa Y, Sugi NH, Nagasu T *et al.* E7070, a novel sulphonamide agent with potent antitumour activity *in vitro* and *in vivo*. *Eur J Cancer* 2001; **37**: 2275–82.
- 5 Raymond E, ten Bokkel Huinink WW, Taieb J *et al.* Phase I and pharmacokinetic study of E7070, a novel chloroindolyl sulfonamide cell-cycle inhibitor, administered as a one-hour infusion every three weeks in patients with advanced cancer. *J Clin Oncol* 2002; **20**: 3508–21.
- 6 Punt CJ, Fumoleau P, van de Walle B, Faber MN, Ravic M, Campone M. Phase I and pharmacokinetic study of E7070, a novel sulfonamide, given at a daily times five schedule in patients with solid tumors. A study by the EORTC-early clinical studies group (ECSG). *Ann Oncol* 2001; **12**: 1289–93.
- 7 Dittrich C, Dumez H, Calvert H *et al.* Phase I and pharmacokinetic study of E7070, a chloroindolyl-sulfonamide anticancer agent, administered on a weekly schedule to patients with solid tumors. *Clin Cancer Res* 2003; **9**: 5195–204.
- 8 Terret C, Zanetta S, Roche H *et al.* Phase I clinical and pharmacokinetic study of E7070, a novel sulfonamide given as a 5-day continuous infusion repeated every 3 weeks in patients with solid tumours. A study by the EORTC Early Clinical Study Group (ECSG). *Eur J Cancer* 2003; **39**: 1097–104.
- 9 Thijssen HH, Flinois JP, Beaune PH. Cytochrome P4502C9 is the

Acknowledgments

We thank Mr Nozomu Koyanagi, Mr Makoto Shiba, Ms. Mayumi Suzuki, Mr Masaki Tanaka, Mr Masakiyo Kato, Mr Yuichi Inai and Dr Tatsuo Watanabe of Eisai Co. for data management and clinical research coordination.

- principal catalyst of racemic acenocoumarol hydroxylation reactions in human liver microsomes. *Drug Metab Dispos* 2000; **28**: 1284–90.
- 10 Van den Bongard HJGD, Sparidans RW, Critchley DJP, Beijnen JH, Schellens JHM. Pharmacokinetic drug-drug interaction of the novel anticancer agent E7070 and acenocoumarol. *Invest New Drugs* 2004; **22**: 151–8.
- 11 Therasse P, Arbutk SG, Eisenhauer EA *et al.* New guidelines to evaluate the response to treatment in solid tumors. European Organization for Research and Treatment of Cancer, National Cancer Institute of the United States, National Cancer Institute of Canada. *J Natl Cancer Inst* 2000; **92**: 205–16.
- 12 Owa T, Yoshino H, Okauchi T *et al.* Discovery of novel antitumor sulfonamides targeting G1 phase of the cell cycle. *J Med Chem* 1999; **42**: 3789–99.
- 13 Rigas JR, Tong WP, Kris MG, Orazem JP, Young CW, Warrell RP Jr. Phase I clinical and pharmacological study of chloroquinoline sulfonamide. *Cancer Res* 1992; **52**: 6619–23.
- 14 Van den Bongard HJGD, Pluim D, van Waardenburg RC, Ravic M, Beijnen JH, Schellens JHM. *In vitro* pharmacokinetic study of the novel anticancer agent E7070: red blood cell and plasma protein binding in human blood. *Anticancer Drugs* 2003; **14**: 405–10.
- 15 Aithal GP, Day CP, Kesteven PJ, Daly AK. Association of polymorphisms in the cytochrome P450 CYP2C9 with warfarin dose requirement and risk of bleeding complications. *Lancet* 1999; **353**: 717–9.
- 16 Takahashi H, Echizen H. Pharmacogenetics of warfarin elimination and its clinical implications. *Clin Pharmacokinet* 2001; **40**: 587–603.
- 17 De Morais SM, Wilkinson GR, Blaisdell J, Meyer UA, Nakamura K, Goldstein JA. Identification of a new genetic defect responsible for the polymorphism of (S)-mephenytoin metabolism in Japanese. *Mol Pharmacol* 1994; **46**: 594–8.
- 18 Mainwaring PN, van Cutsem E, van Laethem JL *et al.* A multicentre randomised phase II study of E7070 in patients with colorectal cancer who have failed 5-fluorouracil based chemotherapy. *Proc Am Soc Clin Oncol* 2002; **21**: 611.



ELSEVIER

LUNG
CANCER



www.elsevier.com/locate/lungcan

Clinical responses of large cell neuroendocrine carcinoma of the lung to cisplatin-based chemotherapy

Shigeo Yamazaki^{a,d}, Ikuo Sekine^{a,*}, Yoshihiro Matsuno^b, Hidefumi Takei^c, Noboru Yamamoto^a, Hideo Kunitoh^a, Yuichiro Ohe^a, Tomohide Tamura^a, Tetsuro Kodama^a, Hisao Asamura^c, Ryosuke Tsuchiya^c, Nagahiro Saijo^a

^a Division of Thoracic Oncology and Internal Medicine, National Cancer Center Hospital, Tsukiji 5-1-1, Chuo-ku, Tokyo 104-0045, Japan

^b Division of Clinical Laboratory, National Cancer Center Hospital, Tokyo

^c Division of Thoracic Surgery, National Cancer Center Hospital, Tokyo

^d Department of Surgery, Keiyu-kai Sapporo Hospital, Sapporo, Japan

Received 30 September 2004; received in revised form 3 January 2005; accepted 3 January 2005

KEYWORDS

Neuroendocrine carcinoma;
Lung cancer;
Chemotherapy;
Cisplatin

Summary

Background: The efficacy of chemotherapy in patients with large cell neuroendocrine carcinoma of the lung (LCNEC) remains unclear.

Methods: Patients with LCNEC who received cisplatin-based chemotherapy were identified by reviewing 567 autopsied and 2790 surgically resected lung cancer patients. The clinical characteristics and objective responses to chemotherapy in these patients were analyzed.

Results: Overall, 20 cases of LCNEC were identified, including stage IIIA ($n=3$), stage IIIB ($n=6$), stage IV ($n=6$) and postoperative recurrence ($n=5$) cases. Six patients had received prior chemotherapy, and 14 were chemo-naïve patients. The patients had received a combination of cisplatin and etoposide ($n=9$), cisplatin, vindesine and mitomycin ($n=6$), cisplatin and vindesine ($n=4$), or cisplatin alone ($n=1$). One patient showed complete response and nine showed partial response, yielding an objective response rate of 50%. The response rate did not differ between patients with the initial diagnosis of SCLC and those with the initial diagnosis of NSCLC, however, the response rate in chemo-naïve patients (64%) was significantly different from that in previously treated patients (17%).

Conclusions: Our results suggest that the response rate of LCNEC to cisplatin-based chemotherapy was comparable to that of SCLC.

© 2005 Elsevier Ireland Ltd. All rights reserved.

* Corresponding author. Tel.: +81 3 3542 2511; fax: +81 3 3542 3815.
E-mail address: isekine@ncc.go.jp (I. Sekine).

1. Introduction

Pulmonary neuroendocrine tumors include a spectrum of four clinicopathological entities classified on the basis of the morphological and biological features: typical carcinoid and atypical carcinoid, which are tumors of low to intermediate grade malignancy, and large cell neuroendocrine carcinoma (LCNEC) and small cell carcinoma (SCLC), which are high-grade malignant tumors. Travis et al. proposed the term LCNEC in 1991 [1], for classifying a type of poorly differentiated high-grade carcinoma characterized by a neuroendocrine appearance under light microscopy. LCNEC exhibits more prominent cellular pleomorphism and higher mitotic activity than the atypical carcinoid (AC), and is distinguished from SCLC by the tumor cell size and chromatin morphology. Although several different terminologies and classifications have been proposed previously, and even the present classification of pulmonary neuroendocrine tumors lacks uniform definition criteria, this class of tumors could become widely accepted and included in the updated histological classification of the World Health Organization [2].

The clinical features of LCNEC have not yet been completely clarified. The prognosis of patients with surgically resected LCNEC is reported to be intermediate between that of AC and SCLC [3–5], and the same as that of resected NSCLC, except that stage I LCNEC has a poorer prognosis than stage I non-small cell lung cancer (NSCLC) [6]. To the best of our knowledge, however, there are no studies that have examined the role of chemotherapy for LCNEC and the prognosis of patients with unresectable LCNEC, even though several reports have been published on the association between response to chemotherapy and the neuroendocrine differentiation of NSCLC [7–9]. The appropriate treatment of unresectable LCNEC, therefore, remains unclear. In the present study, we attempted to investigate the effectiveness of chemotherapy with cisplatin-based regimens for LCNEC in patients with unresectable and recurrent LCNEC.

2. Materials and methods

Eighty-seven of 2790 patients with primary lung cancer who underwent tumor resection from 1982 to 1999 at the National Cancer Center Hospital were found to have tumors with the histological characteristics of LCNEC [6]. Of these, five had received cisplatin-based chemotherapy at the time

of recurrence, and were enrolled as subjects of this study. In addition, 303 of 567 patients who were autopsied from 1983 to 1997 at the National Cancer Center Hospital who had the following histological diagnoses were first selected: SCLC ($n=112$), poorly differentiated adenocarcinoma ($n=99$), large cell carcinoma ($n=58$), poorly differentiated squamous cell carcinoma ($n=29$), poorly differentiated adenosquamous carcinoma ($n=2$), LCNEC ($n=2$), and carcinoid ($n=1$). Of these, 161 had received cisplatin-based chemotherapy were selected for a pathological review. Finally, specimens from 17 of these 161 cases were found to have histological characteristics consistent with the diagnosis of LCNEC, and were selected as subjects of this study. We focused on cisplatin, because since the 1980s, cisplatin has been the only anticancer agent with proven efficacy against both SCLC and NSCLC [10,11]; we, therefore, considered that the effectiveness of chemotherapy for LCNEC could be reasonably evaluated if cisplatin were included in the regimen. Cases which had received adjuvant chemotherapy without evaluable lesions were excluded from the analysis.

All the available paraffin-embedded tissue sections stained with hematoxylin–eosin were reviewed. We classified LCNEC according to the histopathological criteria in the WHO classification [2]. Immunohistochemical analysis was performed to confirm the neuroendocrine features of the tumors. For this purpose, formalin-fixed paraffin sections were stained for a panel of neuroendocrine markers, including chromogranin A (CGA), synaptophysin (SYN), and neural cell adhesion molecule (NCAM), using standard methods. The intensity of immunostaining for these markers was scored as follows: +, when the proportion of stained tumor cells was >50%; ±, when 10–50% of tumor cells were stained; and –, when <10% of tumor cells were stained, as previously described [6]. One case included in this study had the typical histological features of LCNEC, but no neuroendocrine features as determined by the immunohistochemical analysis. For specimens obtained after treatment, we routinely confirmed that the histopathological and morphological features showed no changes due to treatment as compared with the pretreatment biopsy or cytologic specimens. Such cases for which no pretreatment samples were available were excluded from the study; since it has been reported that histological changes may occur after treatment in SCLC [12], we were concerned that misdiagnosis might occur if the same were also true for LCNEC.

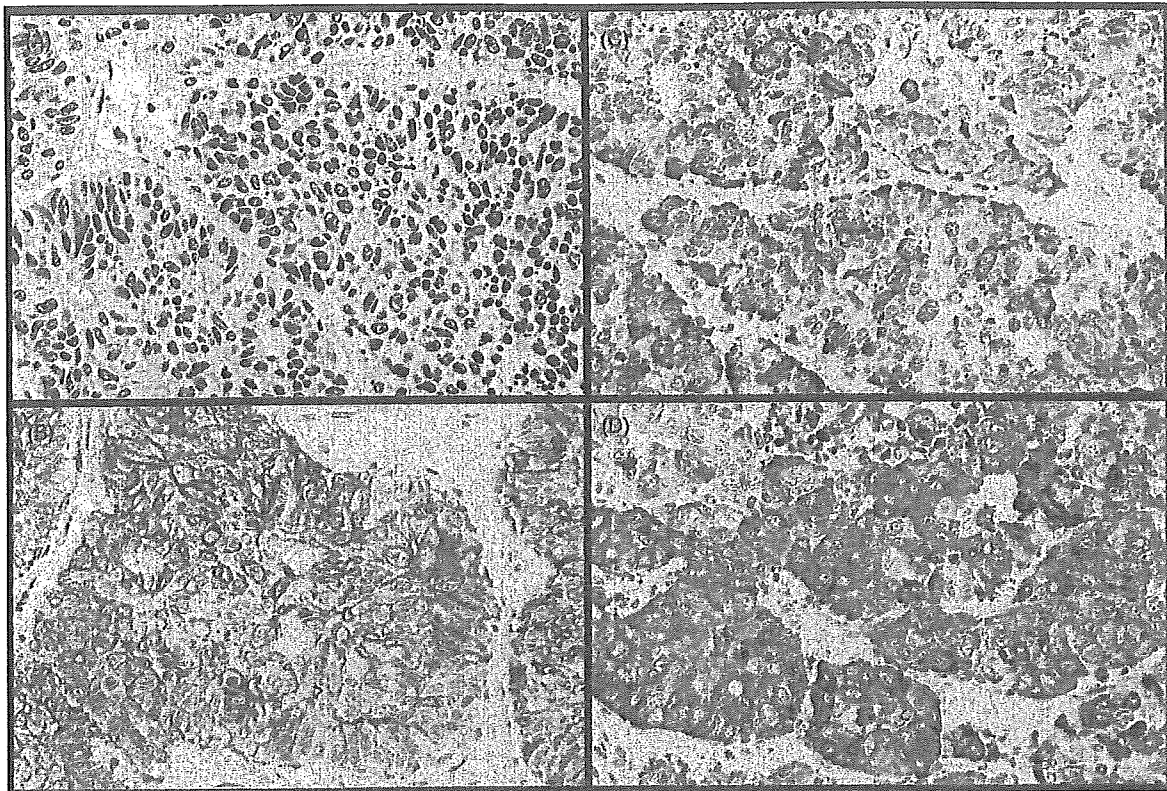


Fig. 1 Case no. 2, 57-year-old man. (A) The tumor cells which are large-sized, polygonal in shape and have a low nuclear-cytoplasmic ratio, are arranged in organoid nests and trabeculae (H&E stain, $\times 200$). Positive staining for neural cell adhesion molecule (B), chromogranin A (C), and synaptophysin (D) (immunostain, $\times 400$).

Clinical information about the cases was obtained from the medical records. The clinical disease staging was reassessed according to the latest International Union Against Cancer (UICC) staging criteria [13]. The response to chemotherapy and overall survival rate were assessed retrospectively. The objective tumor response was evaluated according to the WHO criteria published in 1979 (WHO, 1979) [14]. The survival time was measured from the date of start of chemotherapy with a cisplatin-containing regimen. Survival curves were drawn using the Kaplan–Meier method [15]. Drug toxicity could not be assessed as the study was a retrospective one and records were often incomplete.

3. Results

Overall, 22 cases were recognized as having tumors with histological characteristics consistent with LC-NEC among the autopsied and surgically resected

cases of primary lung cancer that had received cisplatin-based chemotherapy and had evaluable lesions; of these 17 were autopsied cases and five were surgically resected cases. Two of the autopsied cases were excluded, because no pre-treatment pathological or cytological samples were available. The typical microscopic appearance of the tumor specimens is shown in Fig. 1A. The specimen sources for the prechemotherapy-diagnosis included surgically resected specimens ($n=5$), biopsy specimens ($n=9$), and cytology specimens ($n=6$). The histological and cytological findings in the specimens obtained before chemotherapy were consistent with those in the specimens obtained after chemotherapy. We therefore finally enrolled 20 cases in this study. The initial pathologic diagnoses in these patients were as follows: small cell carcinoma ($n=10$), poorly differentiated adenocarcinoma ($n=6$), large cell carcinoma ($n=2$), undifferentiated carcinoma ($n=1$), and poorly differentiated carcinoma ($n=1$) (Table 1). None of the cases had been labeled as LCNEC at the time of initial diagnosis, probably because the concept of LCNEC